

UNCLASSIFIED

AD NUMBER

ADB014346

LIMITATION CHANGES

TO:

Approved for public release; distribution is unlimited.

FROM:

Distribution authorized to U.S. Gov't. agencies only; Test and Evaluation; OCT 1976. Other requests shall be referred to Air Force Armament Lab., Eglin AFB, FL.

AUTHORITY

USADTC ltr, 2 Apr 1980

THIS PAGE IS UNCLASSIFIED

AEDC-TR-76-111

AFATL-TR-76-79

cy.2

001 27 1376

JAN 21 1984

SEP 18 1990



# STATIC STABILITY CHARACTERISTICS OF THE MK-82/84 AIR-INFLATABLE RETARDER HIGH DRAG MODEL

PROPULSION WIND TUNNEL FACILITY  
ARNOLD ENGINEERING DEVELOPMENT CENTER  
AIR FORCE SYSTEMS COMMAND  
ARNOLD AIR FORCE STATION, TENNESSEE 37389

PROPERTY OF U.S. AIR FORCE  
AEDC TECHNICAL LIBRARY

October 1976

## TECHNICAL REPORTS FILE COPY

Final Report for Period 26 - 31 March 1976

This document has been approved for public release  
and its distribution is unlimited. per TAB 80-13

Distribution limited to U.S. Government agencies only; this report contains information on test and evaluation of military hardware; October 1976; other requests for this document must be referred to Air Force Armament Laboratory (AFATL/DLJC), Eglin AFB, FL 32542.

Proprietary Information  
Not to be  
Released Without  
Approval

Prepared for

AIR FORCE ARMAMENT LABORATORY (DLJC)  
EGLIN AIR FORCE BASE, FLORIDA 32542

## NOTICES

When U. S. Government drawings specifications, or other data are used for any purpose other than a definitely related Government procurement operation, the Government thereby incurs no responsibility nor any obligation whatsoever, and the fact that the Government may have formulated, furnished, or in any way supplied the said drawings, specifications, or other data, is not to be regarded by implication or otherwise, or in any manner licensing the holder or any other person or corporation, or conveying any rights or permission to manufacture, use, or sell any patented invention that may in any way be related thereto.

Qualified users may obtain copies of this report from the Defense Documentation Center.

References to named commercial products in this report are not to be considered in any sense as an endorsement of the product by the United States Air Force or the Government.

## APPROVAL STATEMENT

This technical report has been reviewed and is approved for publication.

FOR THE COMMANDER



JOHN C. CARDOSI  
Lt Colonel, USAF  
Chief Air Force Test Director, PWT  
Directorate of Test



ALAN L. DEVEREAUX  
Colonel, USAF  
Director of Test

# UNCLASSIFIED

REPORT DOCUMENTATION PAGE		READ INSTRUCTIONS BEFORE COMPLETING FORM
1 REPORT NUMBER AEDC-TR-76-111 AFATL-TR-76-79	2 GOVT ACCESSION NO.	3 RECIPIENT'S CATALOG NUMBER
4 TITLE (and Subtitle) STATIC STABILITY CHARACTERISTICS OF THE MK-82/84 AIR-INFLATABLE RETARDER HIGH DRAG MODEL	5 TYPE OF REPORT & PERIOD COVERED Final Report, 26 - 31 March 1976	
	6 PERFORMING ORG REPORT NUMBER	
7 AUTHOR(s) R. A. Paulk and C. F. Anderson, ARO, Inc.	8 CONTRACT OR GRANT NUMBER(s)	
9 PERFORMING ORGANIZATION NAME AND ADDRESS Arnold Engineering Development Center (XO) Air Force Systems Command Arnold Air Force Station, TN 37389	10 PROGRAM ELEMENT, PROJECT, TASK AREA & WORK UNIT NUMBERS Program Element 64602F Project 5713 Task 03	
11 CONTROLLING OFFICE NAME AND ADDRESS Air Force Armament Laboratory (AFATL/DLJC) Eglin Air Force Base, FL 32542	12 REPORT DATE October 1976	
	13 NUMBER OF PAGES 64	
14 MONITORING AGENCY NAME & ADDRESS (if different from Controlling Office)	15 SECURITY CLASS (of this report)  UNCLASSIFIED	
	15a DECLASSIFICATION/DOWNGRADING SCHEDULE N/A	
16 DISTRIBUTION STATEMENT (of this Report) Distribution limited to U.S. Government agencies only; this report contains information on test and evaluation of military hardware; October 1976; Other requests for this document must be referred to Air Force Armament Laboratory (AFATL/DLJC), Eglin AFB, FL 32542.		
17 DISTRIBUTION STATEMENT (of the abstract entered in Block 20, if different from Report)		
18 SUPPLEMENTARY NOTES  Available in DDC.		
19 KEY WORDS (Continue on reverse side if necessary and identify by block number) MK-82 bomb                      ordnance MK-84 bomb                      parachutes static stability                retarding Ballutes		
20 ABSTRACT (Continue on reverse side if necessary and identify by block number) An investigation was conducted in the Propulsion Wind Tunnel (16T) to obtain static stability characteristics of the MK-82 and MK-84 with air-inflatable Ballutes <sup>®</sup> and selected fin configu- rations. The MK-82 model was 0.442 scale and had slotted fins with 12.5-deg spin wedges. The MK-84 model was 0.264 scale and had two sets of cambered fins. Each model was equipped with a fuse, lugs, and a lanyard pack. The tests were conducted for various model and Ballute roll orientations at Mach numbers from		

# UNCLASSIFIED

# UNCLASSIFIED

## 20. ABSTRACT (Continued)

0.6 to 1.4 for angles of attack up to 20 deg and Reynolds numbers from  $5.1 \times 10^5$  to  $6.8 \times 10^5$  based on the centerbody maximum diameter. Model and Ballute roll orientation had only small effects on the normal-force, axial-force, and pitching-moment coefficients. Installing the Ballute with the Ballute inlets in the wake of the fins decreased the rolling-moment and yawing-moment coefficients and increased the side-force coefficient.

## PREFACE

The work reported herein was conducted by the Arnold Engineering Development Center (AEDC), Air Force Systems Command (AFSC), for the Air Force Armament Laboratory (AFATL/DLJC) under Program Element 64602F, Project 5713. The AFATL project monitor was Mr. Paul Shirey. The results of the test were obtained by ARO, Inc. (a subsidiary of Sverdrup & Parcel and Associates, Inc.), contract operator of AEDC, AFSC, Arnold Air Force Station, Tennessee. The work was done under ARO Project Number P41T-C7A. The authors of this report were R. A. Paulk and C. F. Anderson, ARO, Inc. The data analysis was completed on April 29, 1976, and the manuscript (ARO Control No. ARO-PWT-TR-76-63) was submitted for publication on June 16, 1976.

## CONTENTS

	<u>Page</u>
1.0 INTRODUCTION . . . . .	5
2.0 APPARATUS	
2.1 Test Facility . . . . .	5
2.2 Test Articles . . . . .	5
2.3 Instrumentation . . . . .	7
3.0 TEST DESCRIPTION	
3.1 Test Procedures and Conditions . . . . .	7
3.2 Precision of Measurements . . . . .	8
4.0 RESULTS	
4.1 MK-82 Bomb . . . . .	9
4.2 MK-84 Bomb . . . . .	10
REFERENCES . . . . .	11

## ILLUSTRATIONS

### Figure

1. Schematic of Model Installation . . . . .	13
2. Photographs of Model Installation . . . . .	14
3. MK-82 Model Details . . . . .	16
4. MK-84 Model Details . . . . .	19
5. Ballute Details . . . . .	22
6. Variation of Reynolds Number and Dynamic Pressure with Mach Number . . . . .	24
7. Axis System and Sign Convention . . . . .	25
8. Effects of Ballute Roll Orientation on the Static Stability Characteristics of the MK-82, $\phi_M = -45$ deg . . . . .	26
9. Effects of Model Roll Orientation on the Static Stability Characteristics of the MK-84 with T2 Fins, $\phi_B = -45$ deg . . . . .	38

<u>Figure</u>		<u>Page</u>
10.	Effects of Fin Configuration on the Static Stability Characteristics of the MK-84, $\phi_B$ and $\phi_M = -45$ deg . . . . .	50
	NOMENCLATURE . . . . .	64



## 1.0 INTRODUCTION

An investigation to determine the six-component static-stability coefficients of the MK-82 and MK-84 bombs with fabric Ballutes® [air-inflatable retarders (AIR)] was conducted in the Propulsion Wind Tunnel (16T), Propulsion Wind Tunnel Facility (PWT). The bombs were tested with selected fin configurations and at various Ballute and tail roll orientations. Data were obtained at Mach numbers from 0.6 to 1.4 at a constant total pressure of 800 psfa. The Reynolds number range, based on center-body maximum diameter, was from  $5.1 \times 10^5$  to  $6.8 \times 10^5$ .

## 2.0 APPARATUS

### 2.1 TEST FACILITY

Tunnel 16T is a closed circuit, continuous flow, variable density wind tunnel capable of operating at Mach numbers between 0.2 and 1.6. The tunnel is equipped with a plenum evacuation system, and the test section is formed by fixed, parallel top and bottom perforated walls, and perforated variable angle side walls. The test section is 16 by 16 ft in cross section and 40 ft long. (A more complete description of the wind tunnel, its operating characteristics, and support equipment is given in Ref. 1.) The location of the test model and the model support system in the test area is indicated in Fig. 1, and photographs of the model installations are shown in Fig. 2.

### 2.2 TEST ARTICLES

#### 2.2.1 MK-82 Bomb Model

Details of the MK-82 test model are shown in Fig. 3. The MK-82 bomb configuration was 0.442 scale and represented the MK-82 warhead and the BSU-49/B stabilizer assembly. The model had a fuse, lugs, lanyard pack, latch, and spring housing. The stabilizer assembly was fitted with four slotted fins equipped with 12.5-deg spin wedges. There were additional fin mounting holes to provide for testing with the fins in the (+) or (x) positions. The lanyard pack, latch, and spring housings

were similarly rotated; however, the lugs remained in the vertical plane. A "whisker"-type boundary-layer trip was located near MS 1.0. The boundary-layer trip was attached to the forebody and consisted of two rows of 0.007-in.-diam copper wires located approximately 0.1 in. apart, protruding approximately one wire diameter. The wires in the second row were staggered relative to the wires in the first row.

### 2.2.2 MK-84 Bomb Model

Details of the MK-84 test model are shown in Fig. 4. The MK-84 bomb configuration was 0.264 scale and represented the MK-84 warhead and the BSU-50/B stabilizer assembly. The model had a fuse, lugs, and lanyard pack.

Two fin configurations, differing in both span and airfoil shape, were used during the test of the MK-84. The fins were cambered to produce a positive static rolling moment. The entire afterbody of the model had to be rotated for testing at different fin roll orientations. The lugs, however, remained in the vertical plane.

The MK-84 and MK-82 had the same forebody, and, therefore, the same "whisker" boundary-layer trip.

### 2.2.3 Ballute (AIR)

Details of the Ballutes are shown in Fig. 5. The Ballute was a ram-air-inflatable spheroid and was attached directly to the model base. In this application it was primarily a decelerator, but it provided some pitch and yaw stabilization as well. In operational use, the Ballute would be contained within the afterbody prior to deployment. However, for these tests the Ballutes were already deployed.

The Ballutes tested were made of fabric and were scale models of the full-size Ballutes, except that no closure plate was attached to the models. Each Ballute was pear shaped, with four scoop inlets and a toroidal

burble fence near its equator. The Ballute attachment to model bases allowed for rotation relative to the model base.

## 2.3 INSTRUMENTATION

Model forces and moments were measured with a six-component, internal strain-gage balance. The model angle of attack was measured with the pitch sector angle-of-attack indicator and was corrected for sting and balance deflections resulting from aerodynamic forces and moments on the model. Electrical signals from the balance and tunnel instrumentation were processed by the PWT data acquisition system and digital computer for online data reduction. Balance outputs were also recorded on an electrostatic recorder for monitoring model dynamic oscillations.

## 3.0 TEST DESCRIPTION

### 3.1 TEST PROCEDURES AND CONDITIONS

Static force and moment data for the MK-82 and MK-84 stores with inflated Ballutes were obtained for Mach numbers from 0.6 to 1.4 for an angle-of-attack range from 0 to 20 deg. MK-82 data were obtained with the fins in the (x) orientation and the Ballute at roll angles of 0 and -45 deg. The lugs were in the vertical plane and were on the windward side as the model was pitched.

MK-84 data were obtained with the fins in the (+) and (x) orientation and the Ballute at a roll angle of -45 deg. The lugs were in the vertical plane and were on the windward side as the model was pitched.

The total pressure was held at 800 psfa, and the variation of Reynolds number and dynamic pressure with Mach number is shown in Fig. 6.

The data were reduced to coefficient form in the aeroballistic axis system with the moment reference at MS 15.416 for the MK-82 model and at MS 13.166 for the MK-84 model. The axis system and sign convention are presented in Fig. 7.

## 3.2 PRECISION OF MEASUREMENTS

### 3.2.1 Test Conditions

The uncertainties in angle of attack and roll angle are  $\pm 0.06$  deg and  $\pm 0.10$  deg, respectively. The estimated uncertainties in the tunnel Mach number and tunnel dynamic pressure are given in the following table and are based on a 95-percent probability.

	Mach Number						
	0.6	0.8	0.9	1.0	1.1	1.2	1.4
$\Delta M_{\infty}$	0.002	0.003	0.004	0.005	0.007	0.008	0.012
$\Delta q_{\infty}$	1.230	1.930	2.540	3.200	3.960	4.680	5.700

### 3.2.2 Aerodynamic Coefficients

The estimated uncertainties in the aerodynamic coefficients for the MK-82 and MK-84 bombs are given in the following tables are based on a 95-percent probability.

	MK-82 Mach Number					
	0.6	0.8	0.9	1.0	1.1	1.2
$\Delta C_N$	0.184	0.125	0.115	0.114	0.124	0.123
$\Delta C_Y$	0.149	0.101	0.089	0.081	0.075	0.071
$\Delta C_A$	0.252	0.173	0.179	0.223	0.267	0.257
$\Delta C_{\ell}$	0.072	0.048	0.042	0.039	0.036	0.034
$\Delta C_m$	0.242	0.173	0.200	0.257	0.332	0.331
$\Delta C_n$	0.186	0.126	0.110	0.101	0.093	0.089

	MK-84 Mach Number						
	0.6	0.8	0.9	1.0	1.1	1.2	1.4
$\Delta C_N$	0.183	0.123	0.109	0.102	0.097	0.094	0.083
$\Delta C_Y$	0.150	0.100	0.089	0.080	0.075	0.071	0.068
$\Delta C_A$	0.243	0.165	0.149	0.141	0.139	0.134	0.112
$\Delta C_\ell$	0.071	0.048	0.042	0.038	0.036	0.034	0.033
$\Delta C_m$	0.230	0.155	0.141	0.137	0.136	0.131	0.105
$\Delta C_n$	0.187	0.125	0.110	0.100	0.093	0.089	0.085

## 4.0 RESULTS

### 4.1 MK-82 BOMB

The effects of Ballute roll orientation on the static stability characteristics of the MK-82 model at -45 deg roll are shown in Fig. 8 for all Mach numbers of interest. Normal-force and pitching-moment coefficients had slightly larger absolute values for the  $\phi_B = 0$  configuration than for the  $\phi_B = -45$  deg configuration. The axial-force coefficients were nearly equal for both Ballute roll orientations for subsonic Mach numbers. For  $M_\infty = 1.1$  the  $\phi_B = 0$  configuration had a higher axial-force coefficient.

The fin spin wedges generated a positive rolling moment on the MK-82 model, as is shown in Ref. 2. Adding the Ballute produced a negative model rolling-moment coefficient for both Ballute roll orientations for  $M_\infty = 0.6$ . For higher Mach numbers, only the  $\phi_B = -45$  deg configuration (Ballute inlets in line with fins) produced a negative model rolling-moment coefficient.

The side-force coefficient generally tended to decrease with increasing angle of attack while the yawing-moment coefficient increased. Both side-force and yawing-moment coefficients generally showed a break or change in slope at  $\alpha = 9$  deg. The reason for this change in slope is

not readily apparent; however, it should be noted that the Ballute stayed approximately aligned with the airflow as angle of attack increased. Therefore, the changes observed at  $\alpha = 9$  deg could have been produced by the Ballute's moving into the vortices being shed by the forebody. Rolling the Ballute to  $\phi_B = -45$  deg (inlets aligned with the fins) generally reversed the side-force and yawing-moment coefficients.

## 4.2 MK-84 BOMB

The MK-84 was tested with the ballute at  $-45$  deg roll orientation for all test conditions. The effects of fin roll orientation on the static stability characteristics of the MK-84 with T2 fins are shown in Fig. 9. The configuration with the fins in the (+) orientation had the largest absolute values of normal-force and pitching-moment coefficient. The axial-force coefficient was largest for the model with (+) fin orientation for  $M_\infty = 0.6, 0.8,$  and  $0.9$ . For  $M_\infty = 1.1$ , the axial-force coefficients were nearly equal for both fin orientations. When the Ballute inlets were aligned with the fins ( $\phi_M = -45$  deg), the rolling-moment coefficient was either reduced or negative.

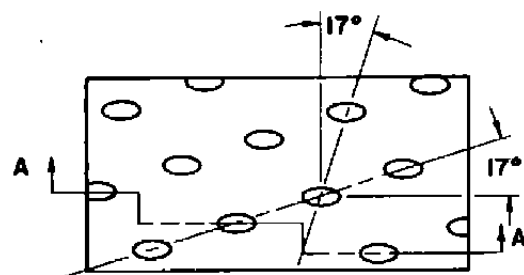
The side-force coefficient generally tended to decrease with increasing angle of attack, whereas the yawing-moment coefficient increased, as was the case for the MK-82. The side-force coefficient was generally larger and the yawing-moment coefficient was generally smaller for the case with the fins and Ballute inlets aligned,  $\phi_M = -45$  deg.

The effect of fin size and camber on the static stability characteristics of the MK-84 store is shown in Fig. 10. For  $\alpha < 6$  deg, the T3 fins produced slightly larger absolute values of normal-force and pitching-moment coefficients than the T2 fins. For higher angles of attack, the two sets of fins produced nearly equal normal-force and pitching-moment coefficients. The axial-force coefficients were nearly the same for both configurations.

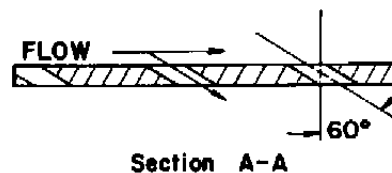
The T3 fins produced a larger side-force coefficient and a smaller yawing-moment coefficient than did the T2 fins. The T3 fins produced a larger rolling-moment coefficient than did the T2 fins.

## REFERENCES

1. Test Facilities Handbook (Tenth Edition). "Propulsion Wind Tunnel Facility, Vol. 4." Arnold Engineering Development Center, May 1974.
2. Anderson, C. F. and Carleton, W. E. "Static and Dynamic Stability Characteristics of the Fixed-Fin and Inflatable Stabilizer Retarder Configurations of the MK-82 Store at Transonic Speeds." AEDC-TR-75-149 (AD-B007733L), November 1975.



TYPICAL PERFORATED  
WALL PATTERN



6% Open Area  
Hole Diameter = 0.75 in.  
Plate Thickness = 0.75 in.

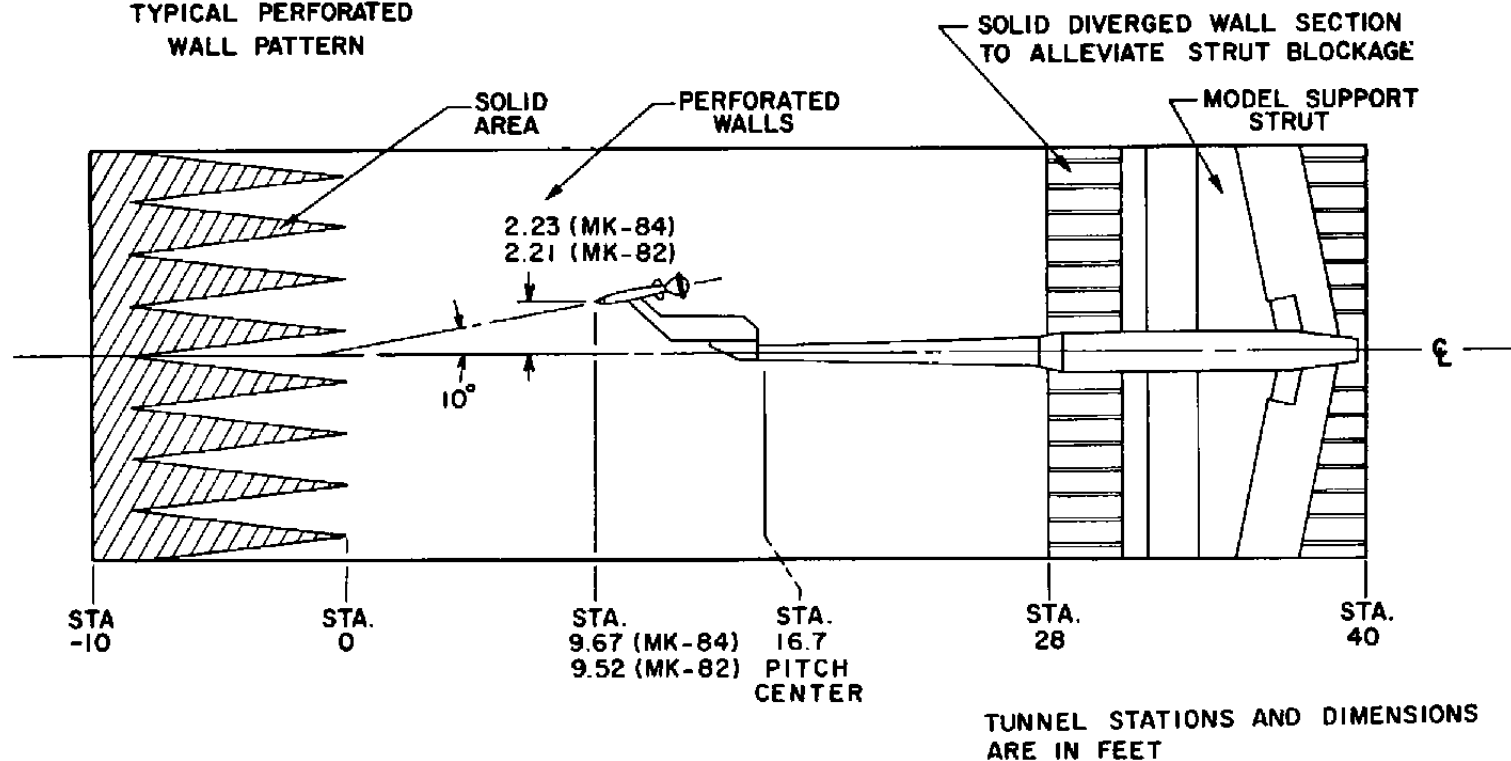


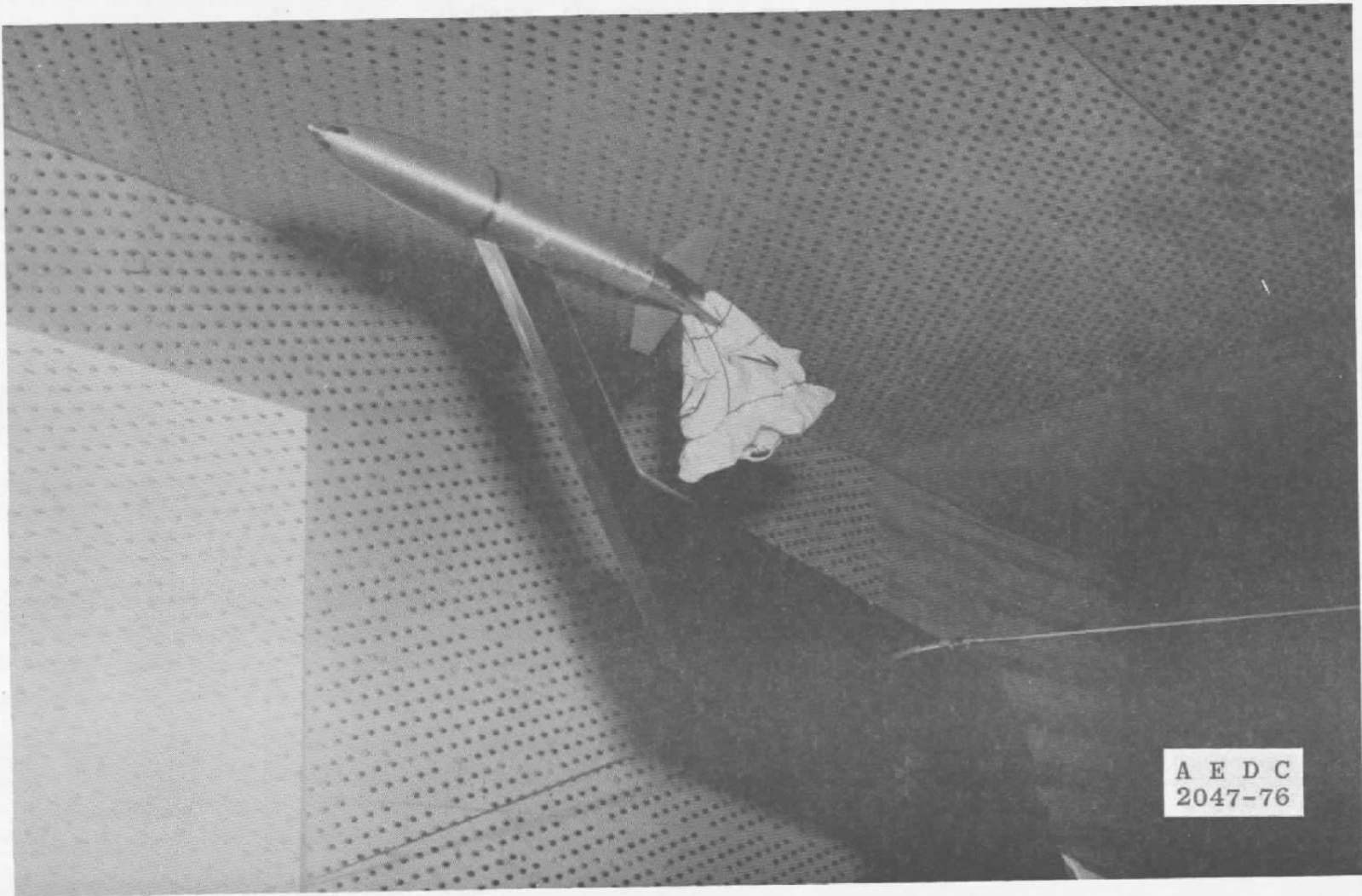
Figure 1. Schematic of model installation.



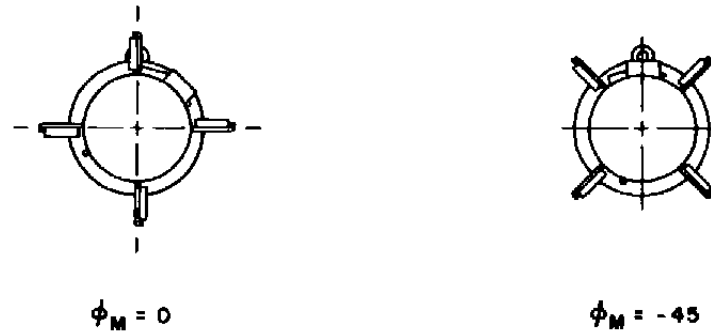
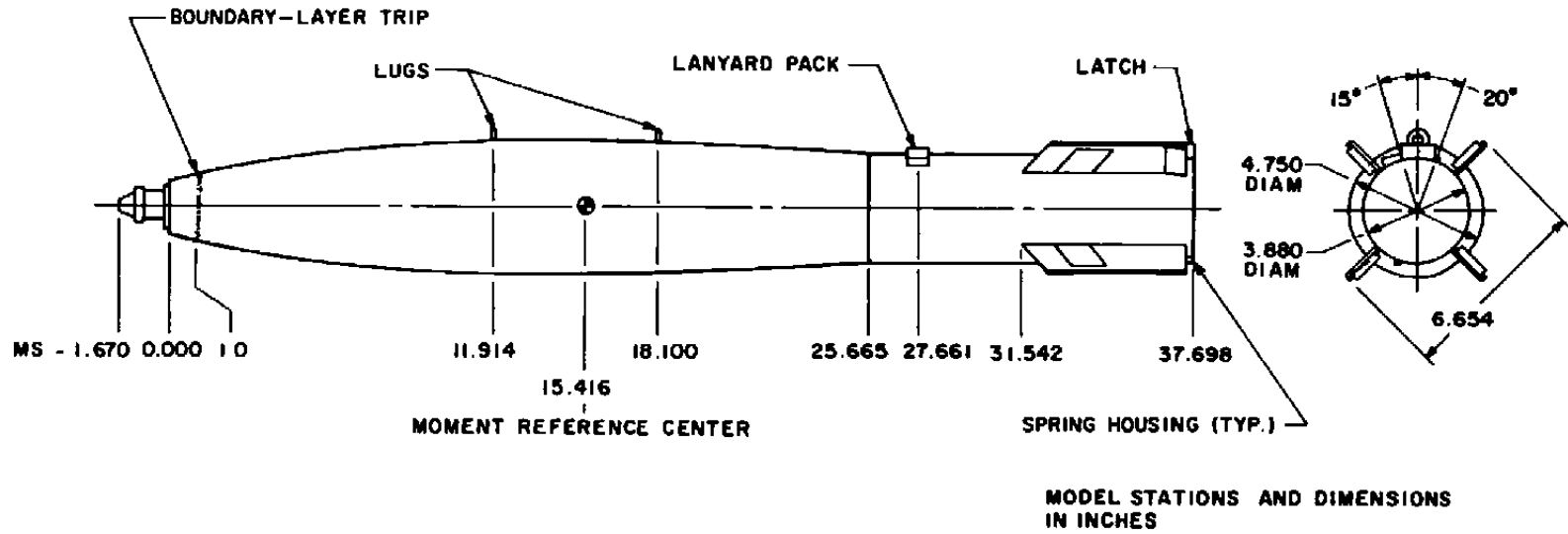


a. MK-82

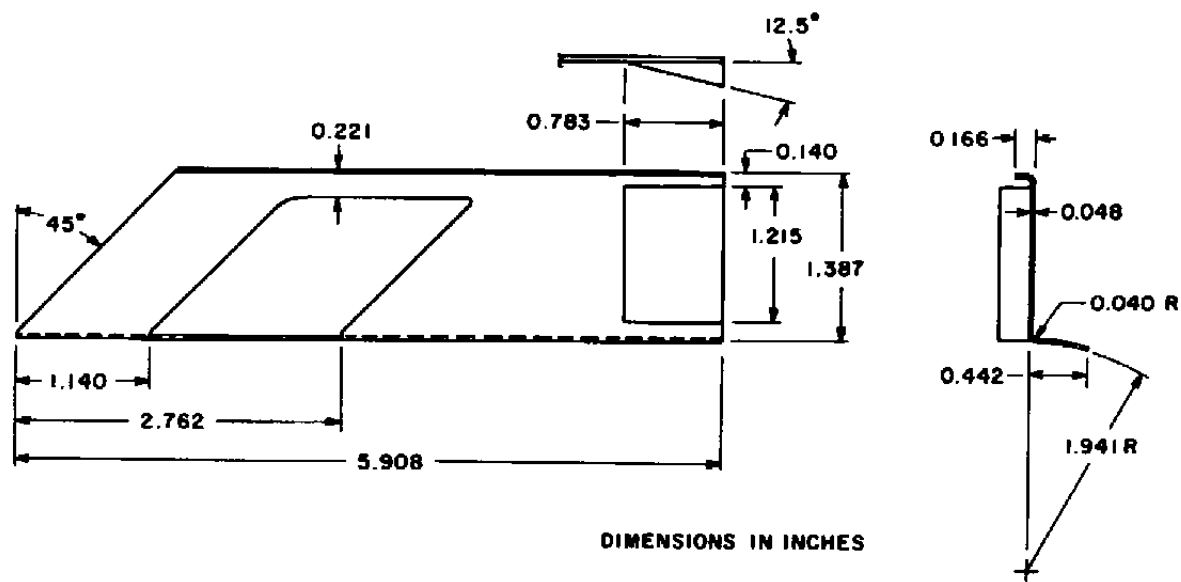
Figure 2. Photographs of model installation.



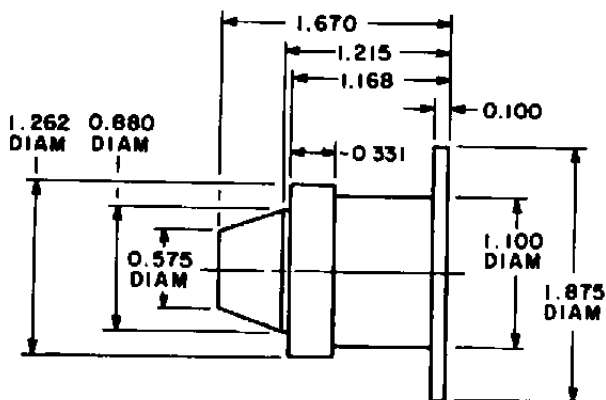
b. MK-84  
Figure 2. Concluded.



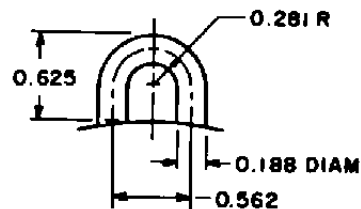
a. Model dimensions and fin orientation  
Figure 3. MK-82 model details.



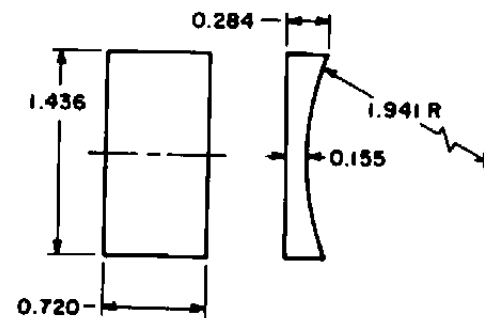
b. Fin dimensions  
Figure 3. Continued.



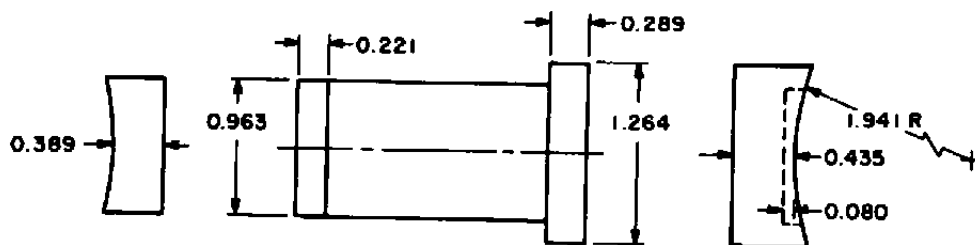
FUZE



LUGS



LANYARD PACK



LATCH



TOP

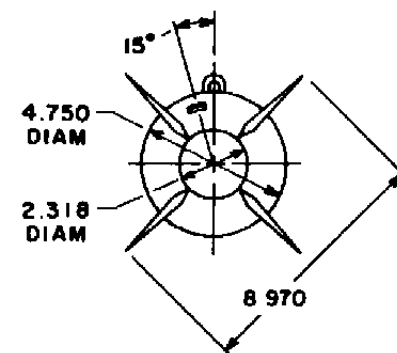
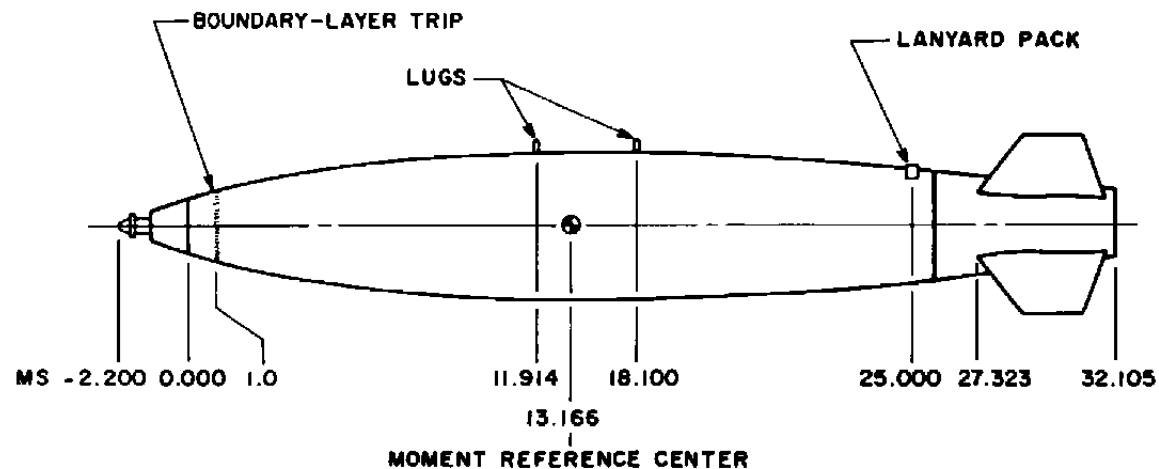


BOTTOM

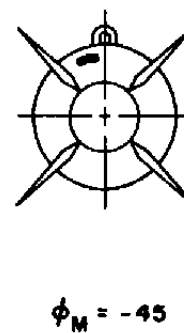
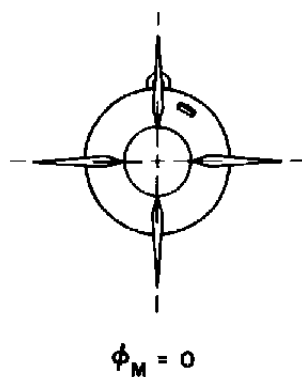
SPRING HOUSING

DIMENSIONS IN INCHES

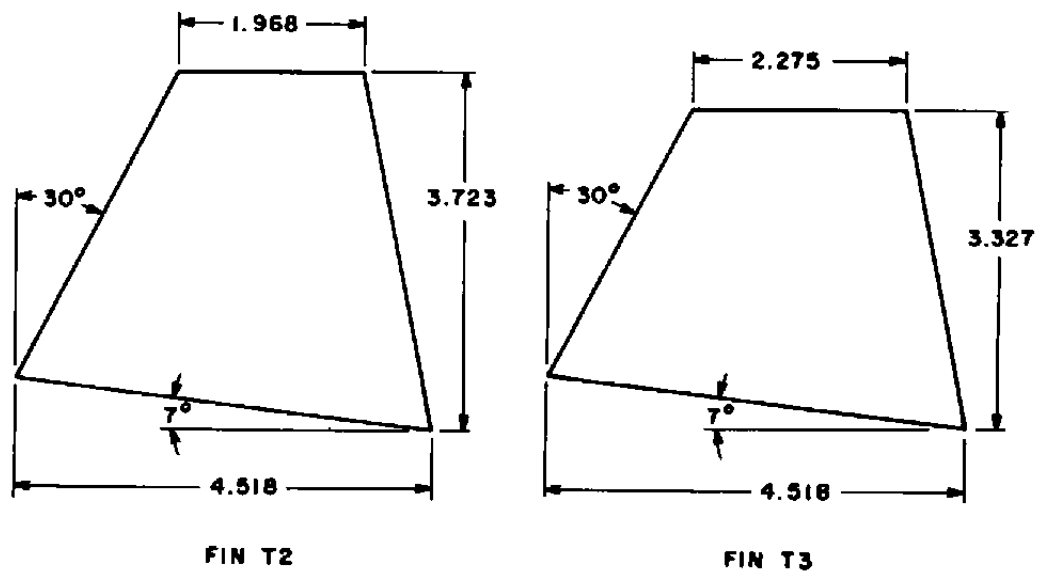
c. External component dimensions  
Figure 3. Concluded.



MODEL STATIONS AND DIMENSIONS  
IN INCHES

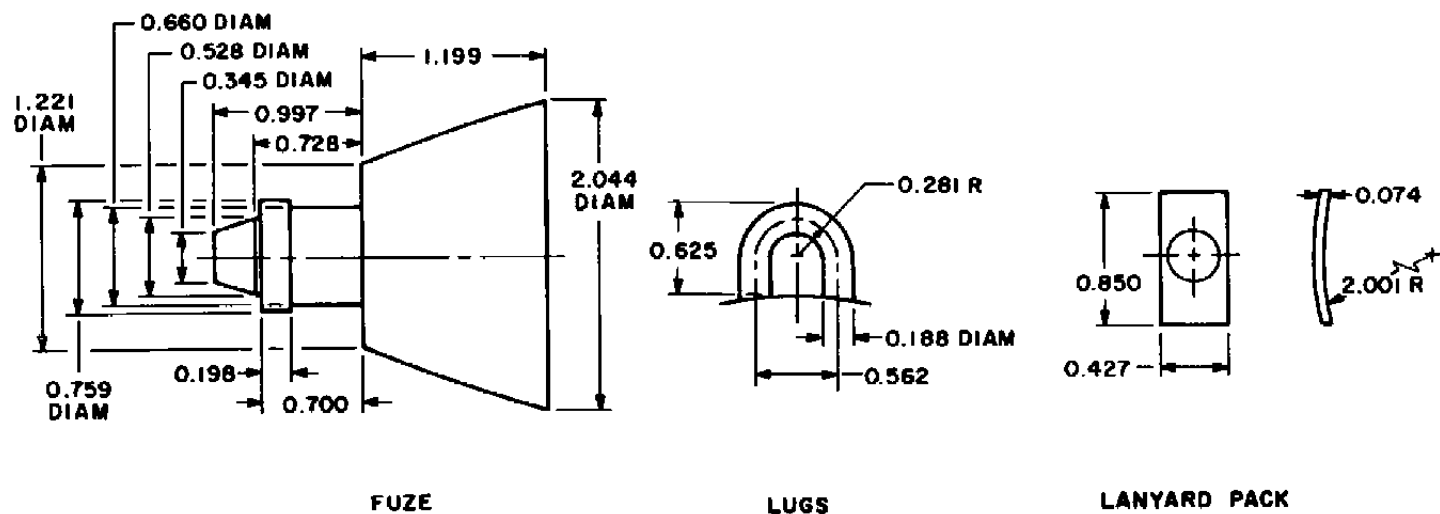


a. Model dimensions and fin orientation  
Figure 4. MK-84 model details.



DIMENSIONS IN INCHES

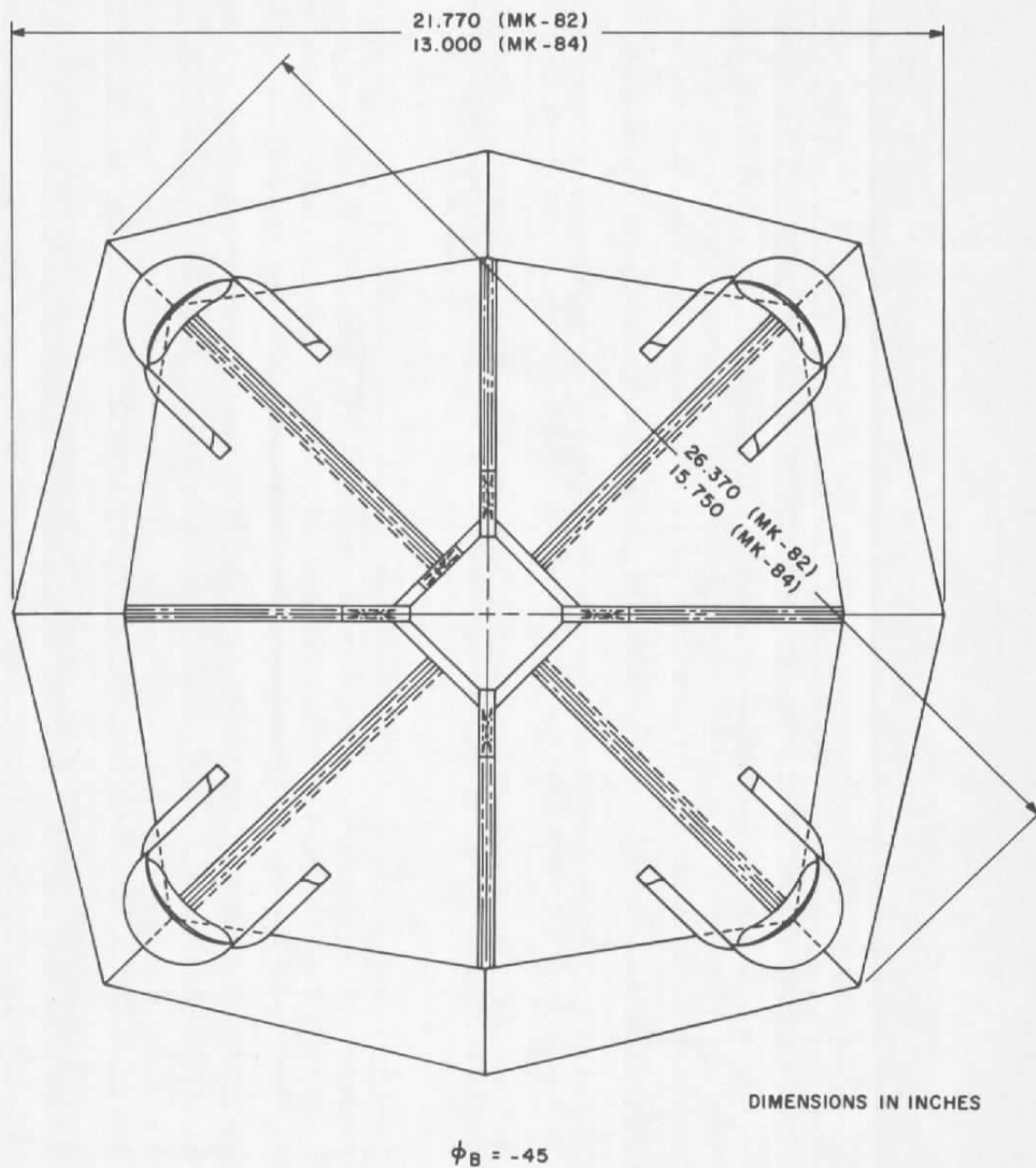
b. Fin dimensions and identification  
Figure 4. Continued.



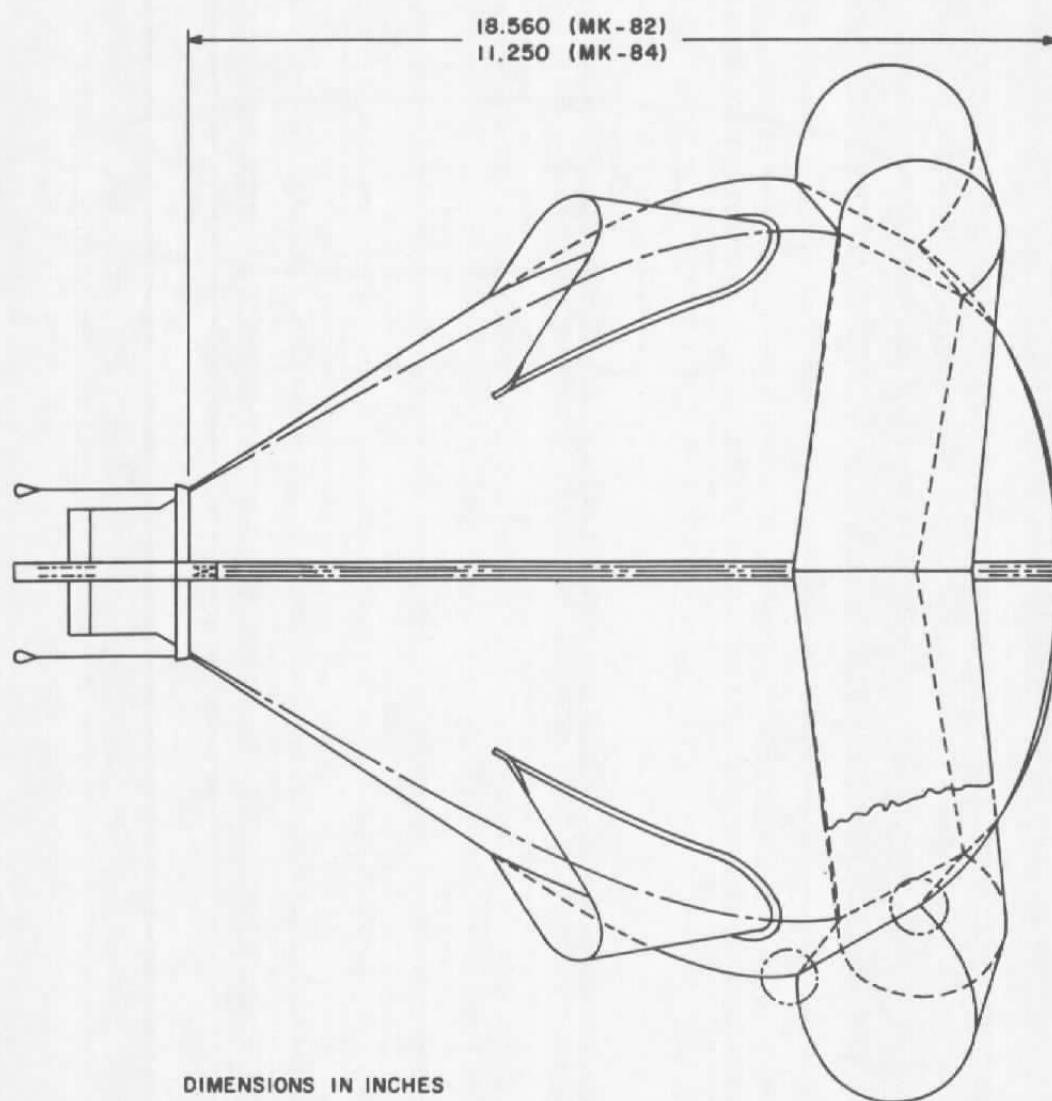
DIMENSIONS IN INCHES

c. External component dimensions  
Figure 4. Concluded.





a. Front view showing ballute dimensions and roll orientation  
Figure 5. Ballute details.



DIMENSIONS IN INCHES

b. Side view showing ballute dimensions  
Figure 5. Concluded.

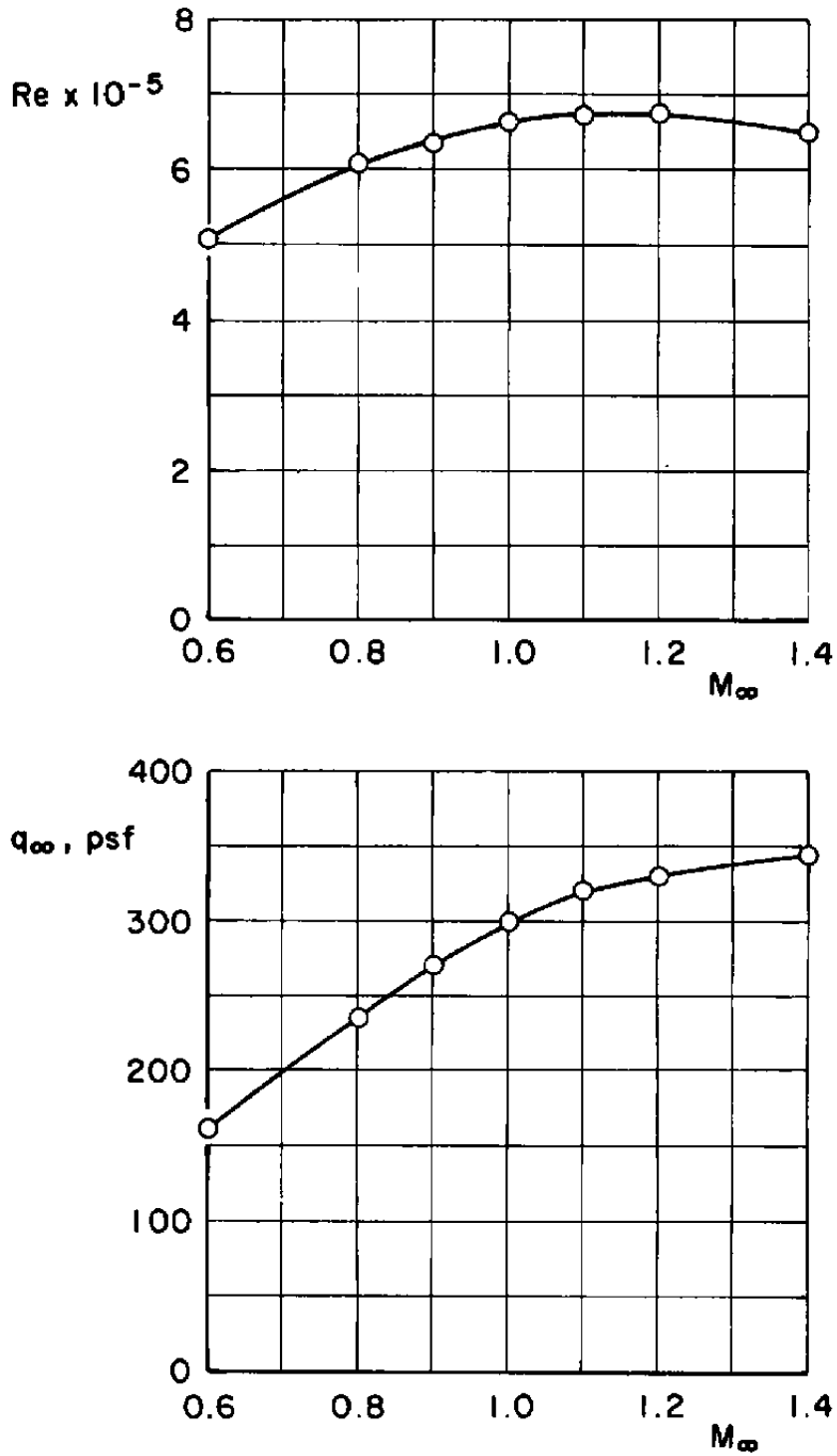
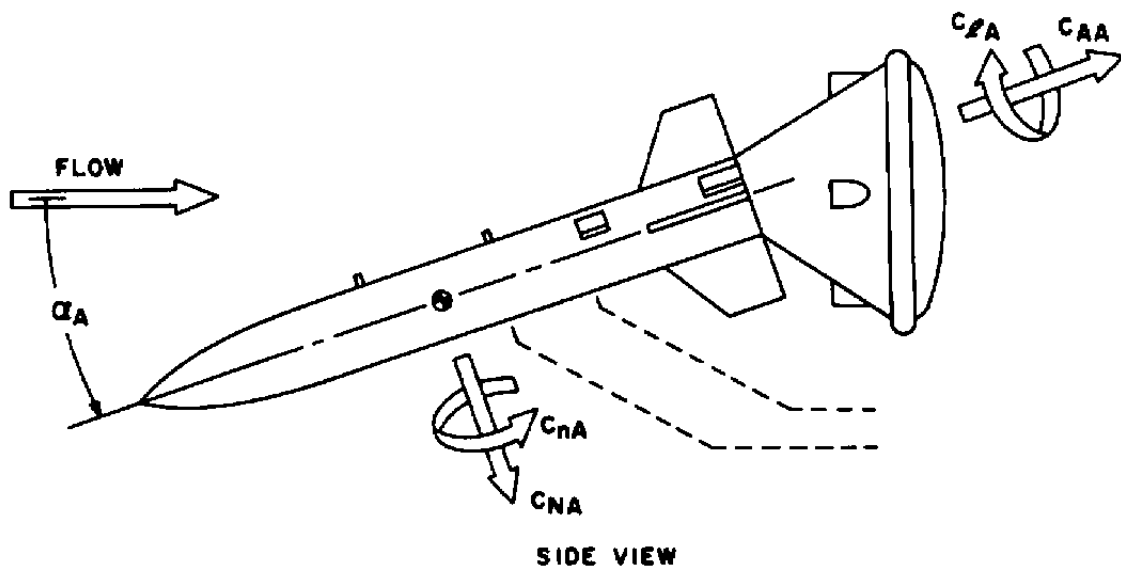


Figure 6. Variation of Reynolds number and dynamic pressure with Mach number.



ARROWS INDICATE POSITIVE DIRECTION  
OF FORCES, MOMENTS AND ANGLES

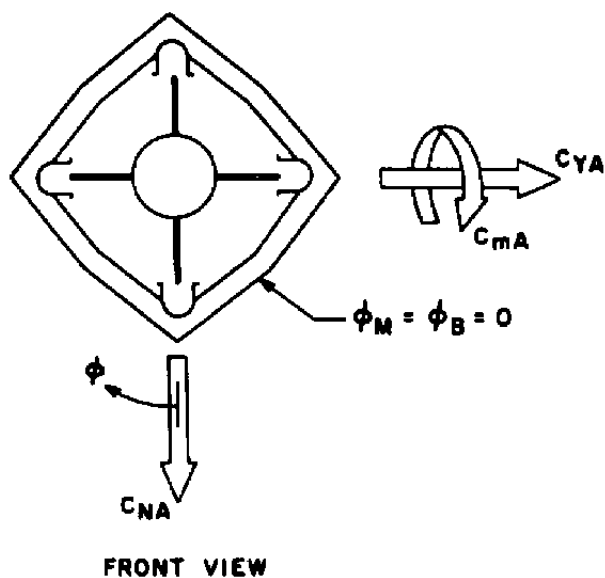
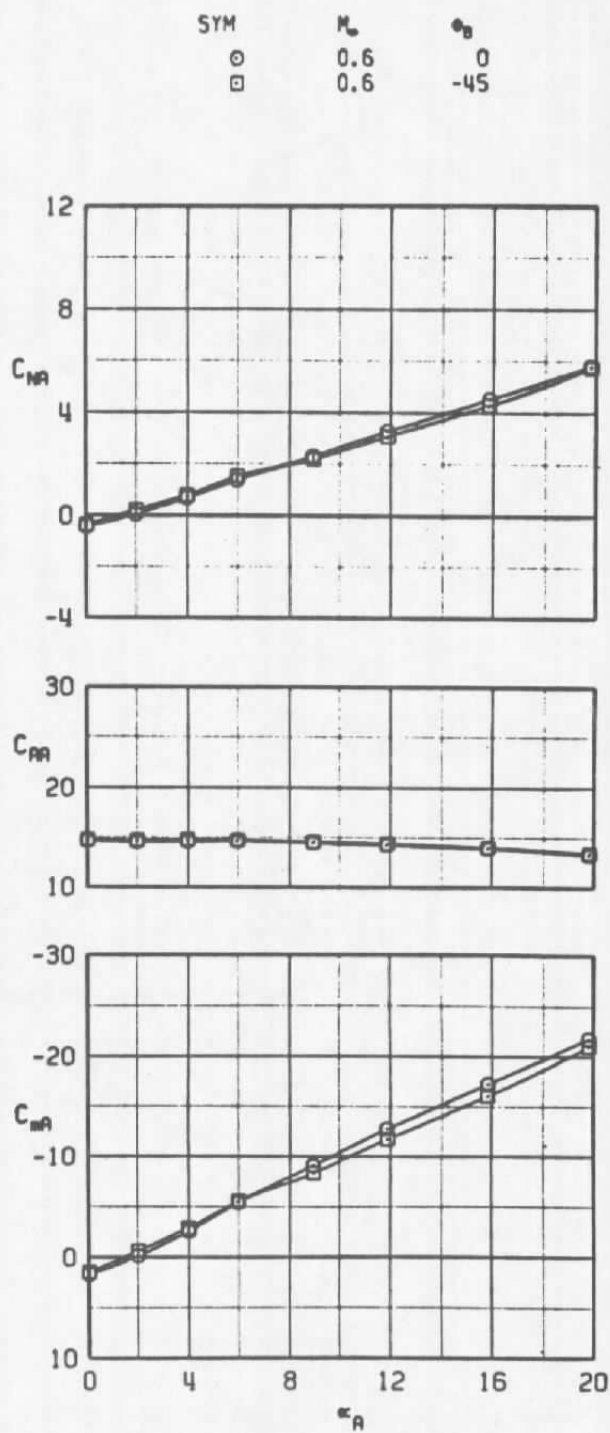


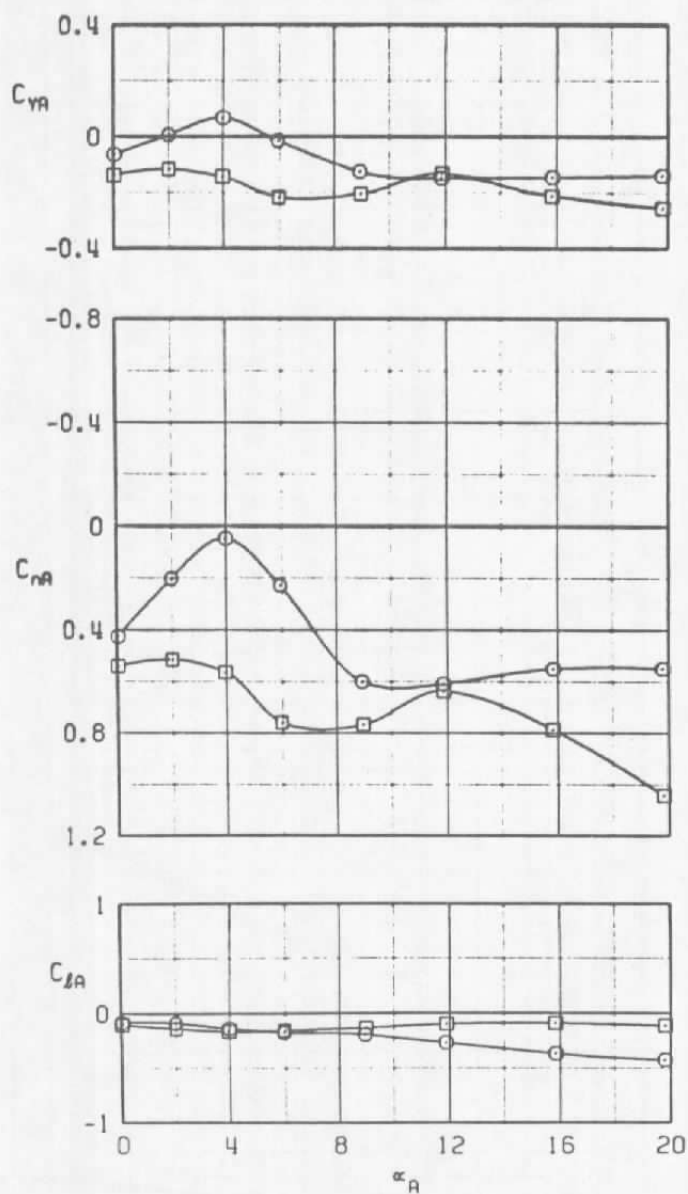
Figure 7. Axis system and sign convention.



a.  $M_\infty = 0.6$

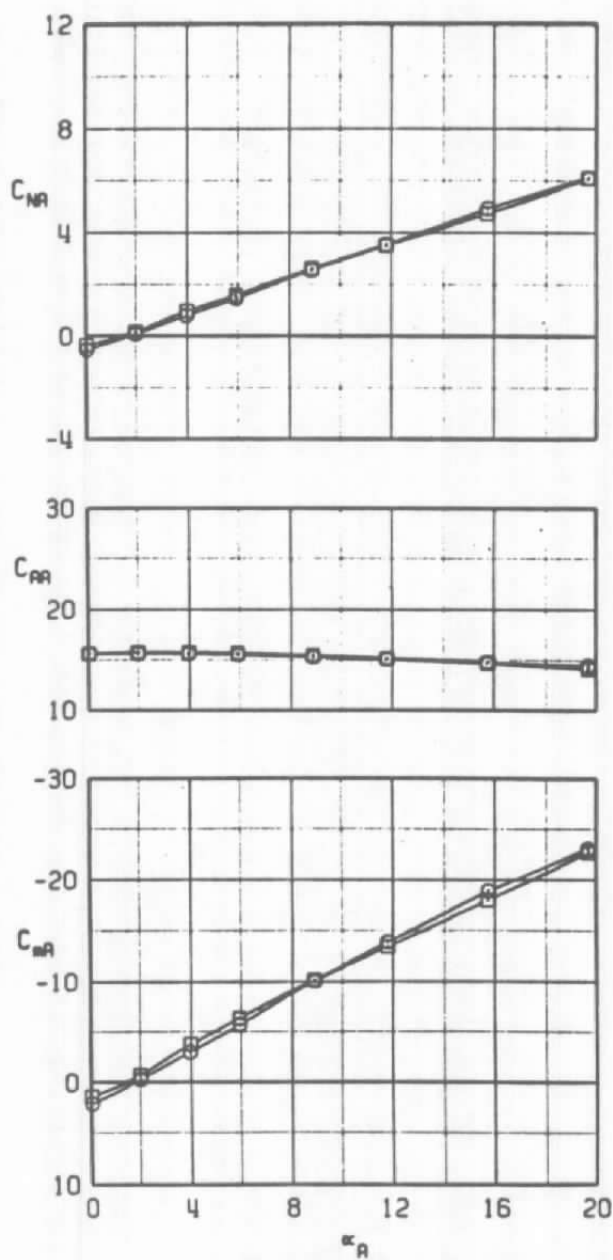
Figure 8. Effects of ballute roll orientation on the static stability characteristics of the MK-82,  $\phi_M = -45$  deg.

SYM	$M_\infty$	$\phi_0$
○	0.6	0
□	0.6	-45



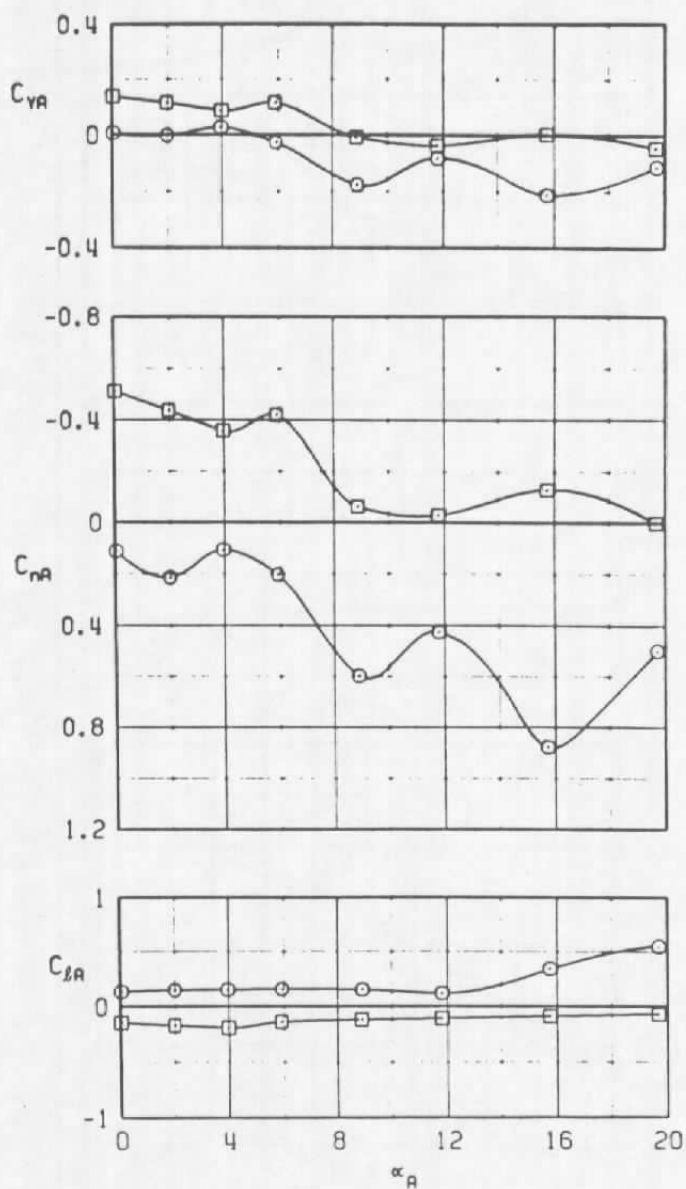
a. Concluded  
Figure 8. Continued.

SYM	$M_\infty$	$\phi_\theta$
○	0.8	0
□	0.8	-45



b.  $M_\infty = 0.8$   
Figure 8. Continued.

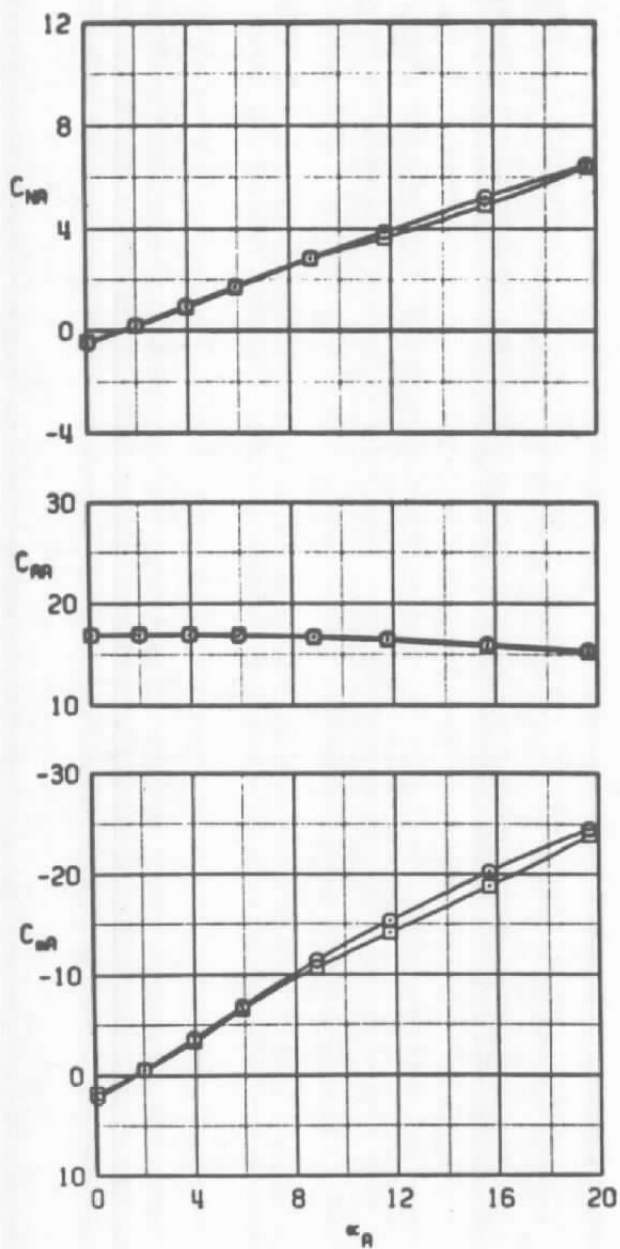
SYM	$M_\infty$	$\phi_B$
○	0.8	0
□	0.8	-45



b. Concluded  
Figure 8. Continued.

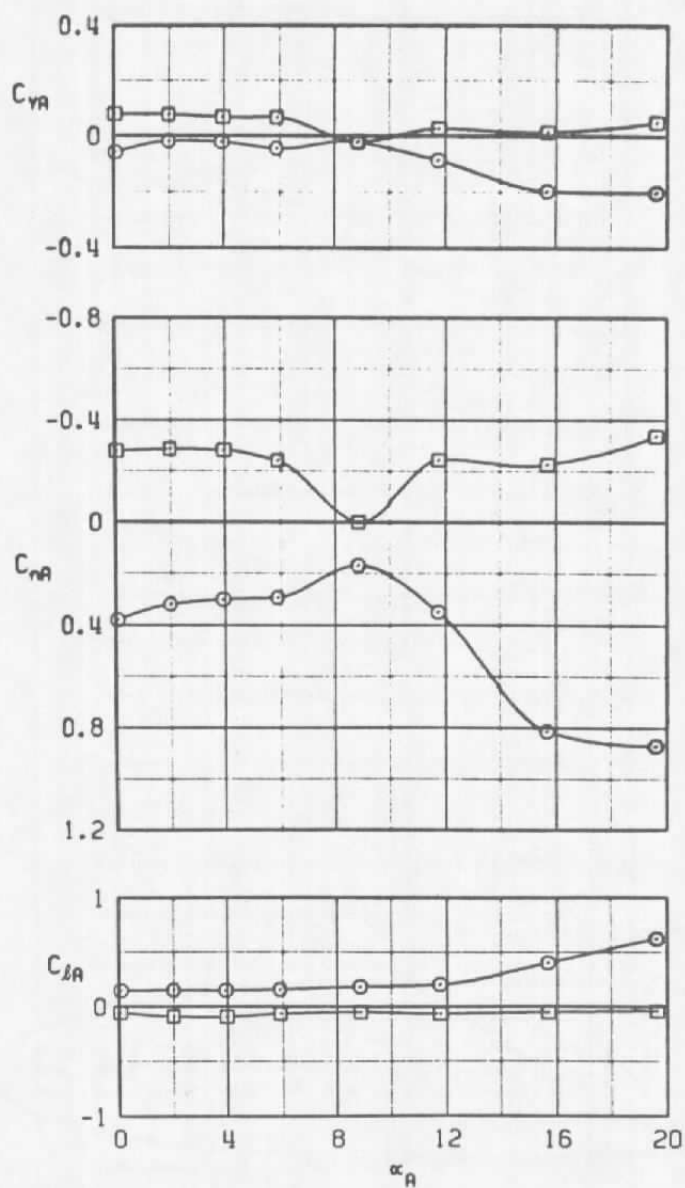


SYM	$M_\infty$	$\alpha$
○	0.9	0
□	0.9	-45



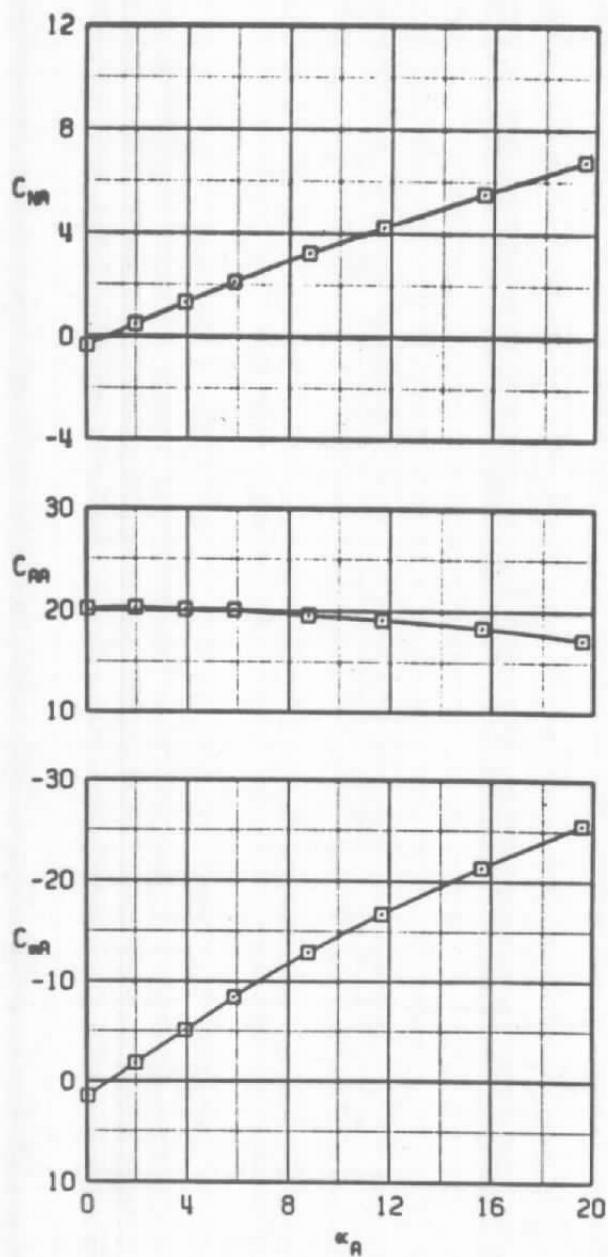
c.  $M_\infty = 0.9$   
Figure 8. Continued.

SYM	$M_\infty$	$\phi_\theta$
○	0.9	0
□	0.9	-45



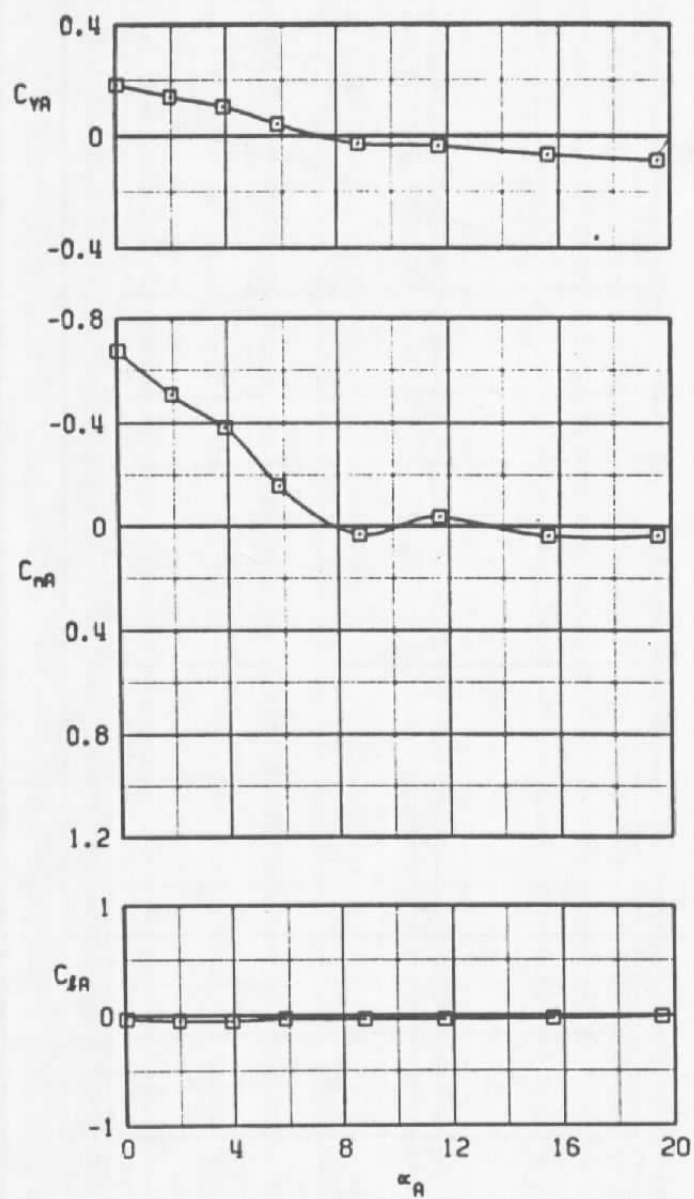
c. Concluded  
Figure 8. Continued.

SYM  $M_\infty$   $\alpha_R$   
 □ 1.0 -45



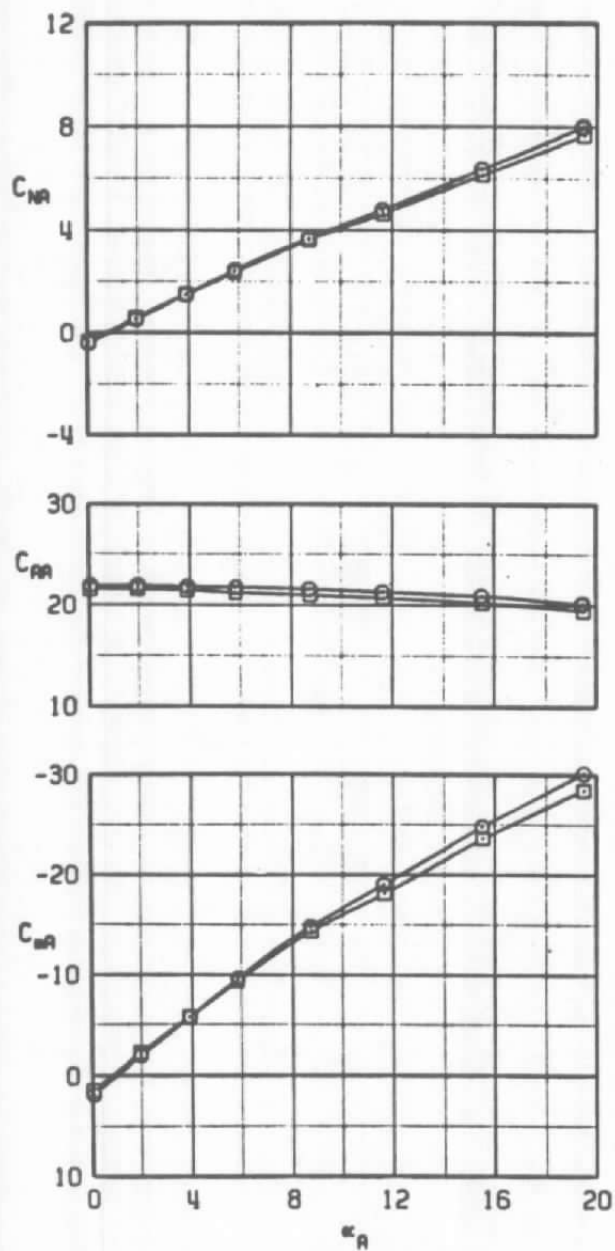
d.  $M_\infty = 1.0$   
 Figure 8. Continued.

SYM       $M_\infty$        $\phi_B$   
 □      1.0      -45



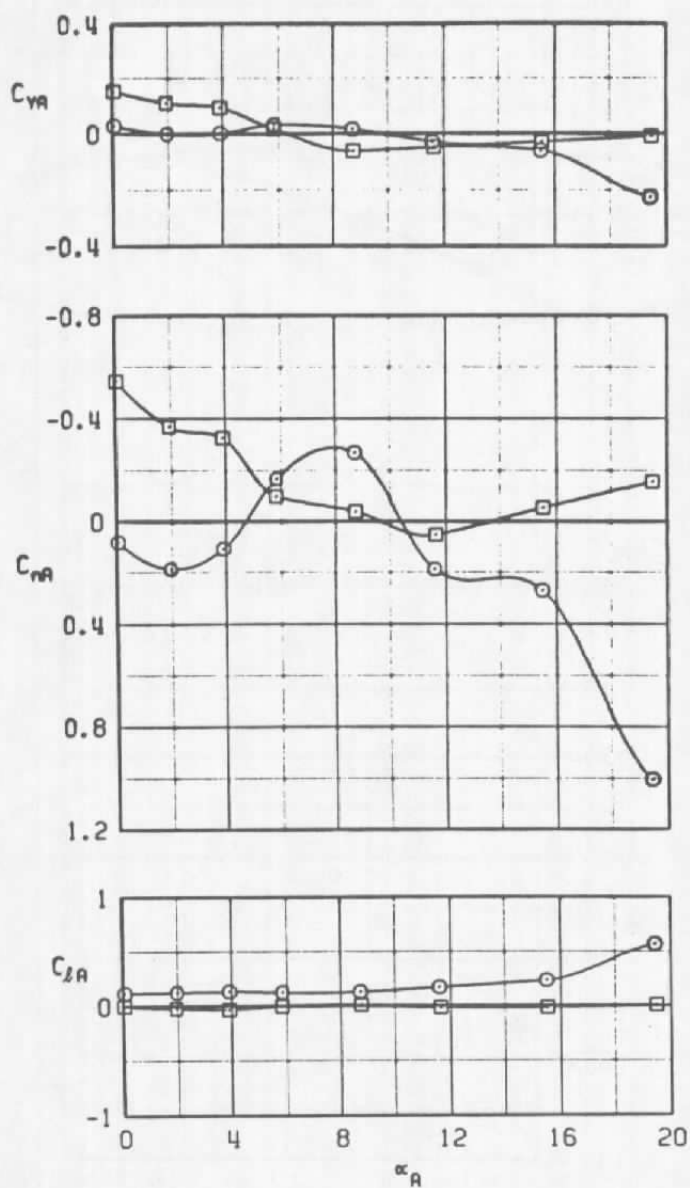
d. Concluded  
 Figure 8. Continued.

SYM	$M_\infty$	$\phi_B$
○	1.1	0
□	1.1	-45



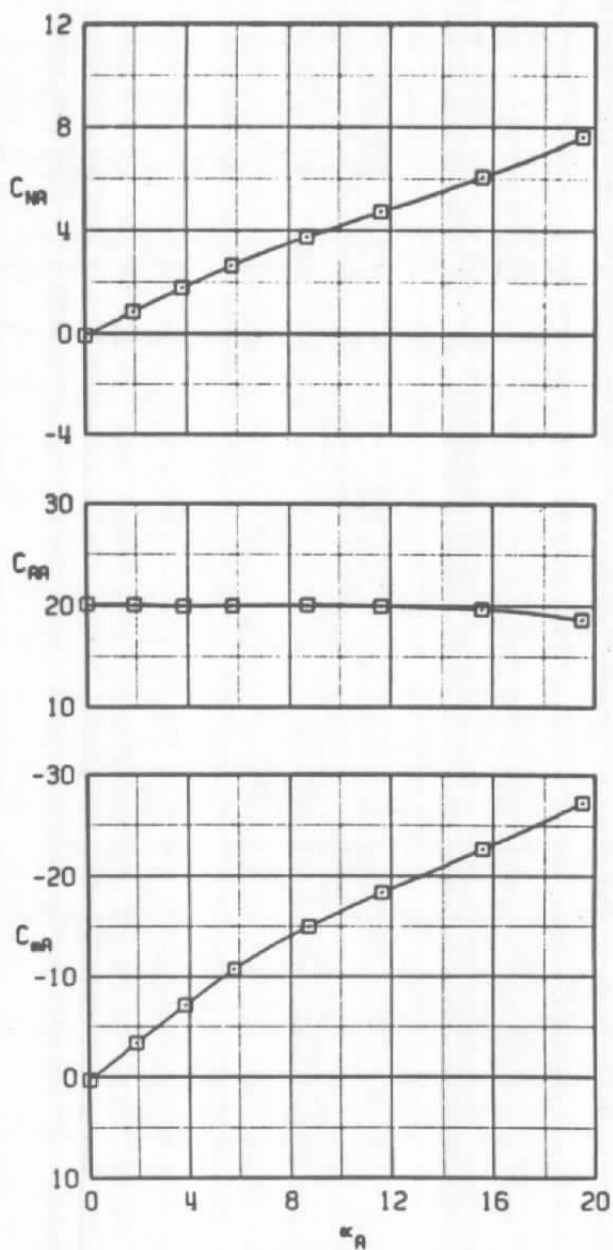
e.  $M_\infty = 1.1$   
Figure 8. Continued.

SYM	$M_\infty$	$\phi_B$
○	1.1	0
□	1.1	-45



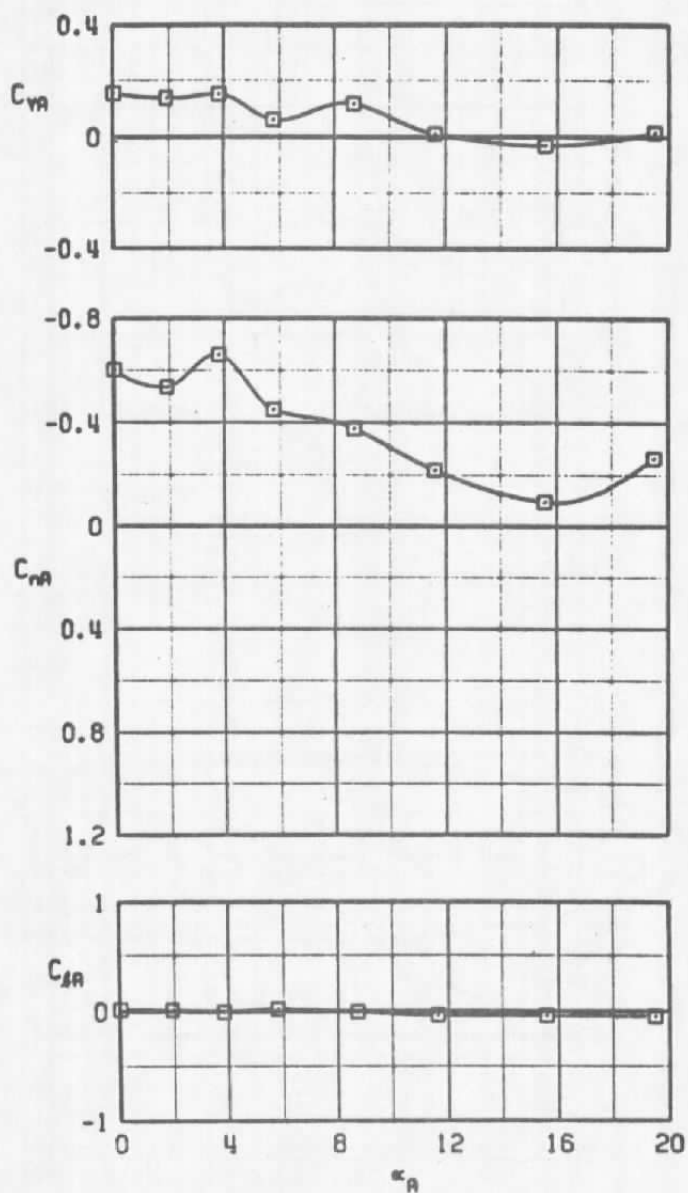
e. Concluded  
Figure 8. Continued.

SYM  $M_\infty$   $\theta$   
 □ 1.2 -45



f.  $M_\infty = 1.2$   
 Figure 8. Continued.

SYM  $M_\infty$   $\alpha$   
 □ 1.2 -45



f. Concluded  
 Figure 8. Concluded.



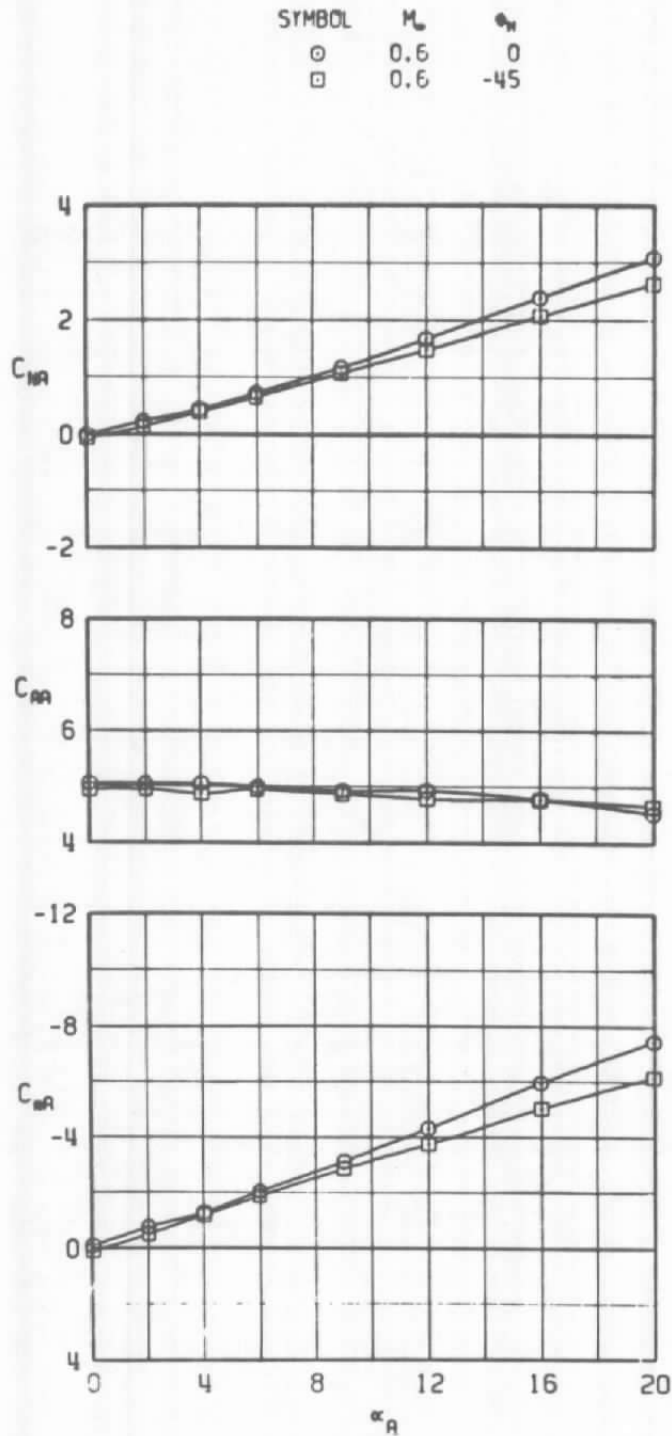
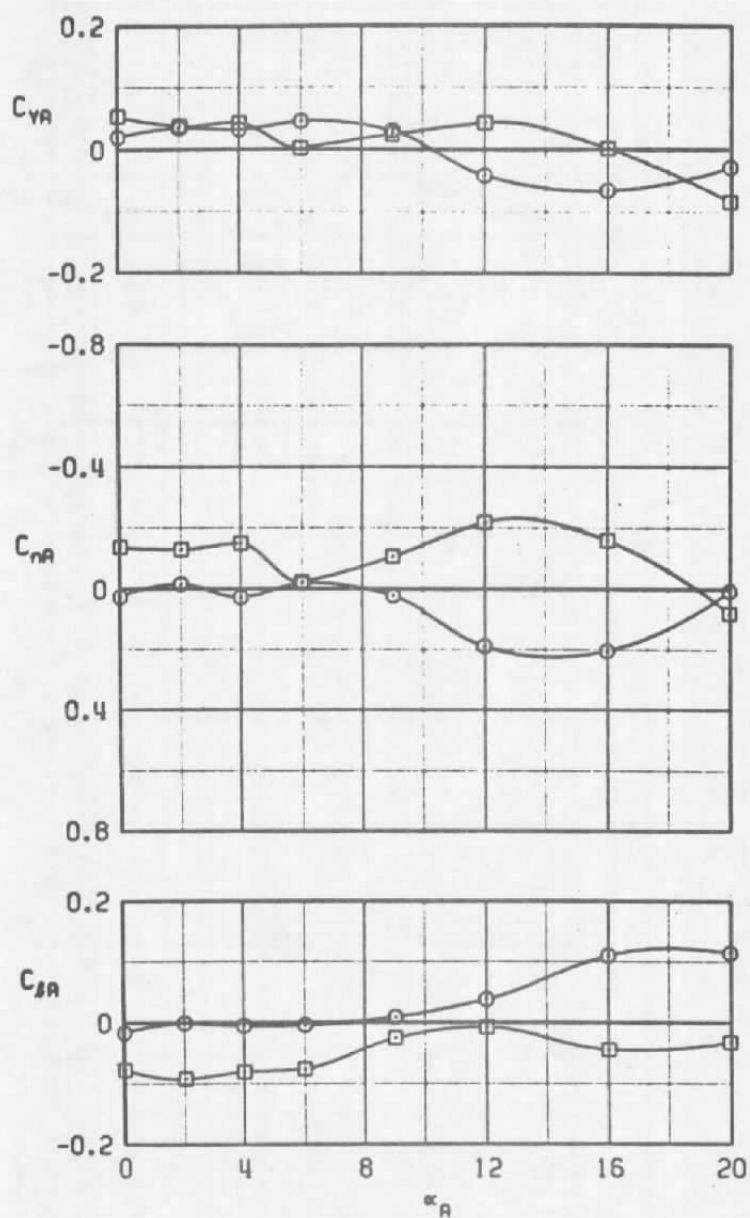
a.  $M_\infty = 0.6$ 

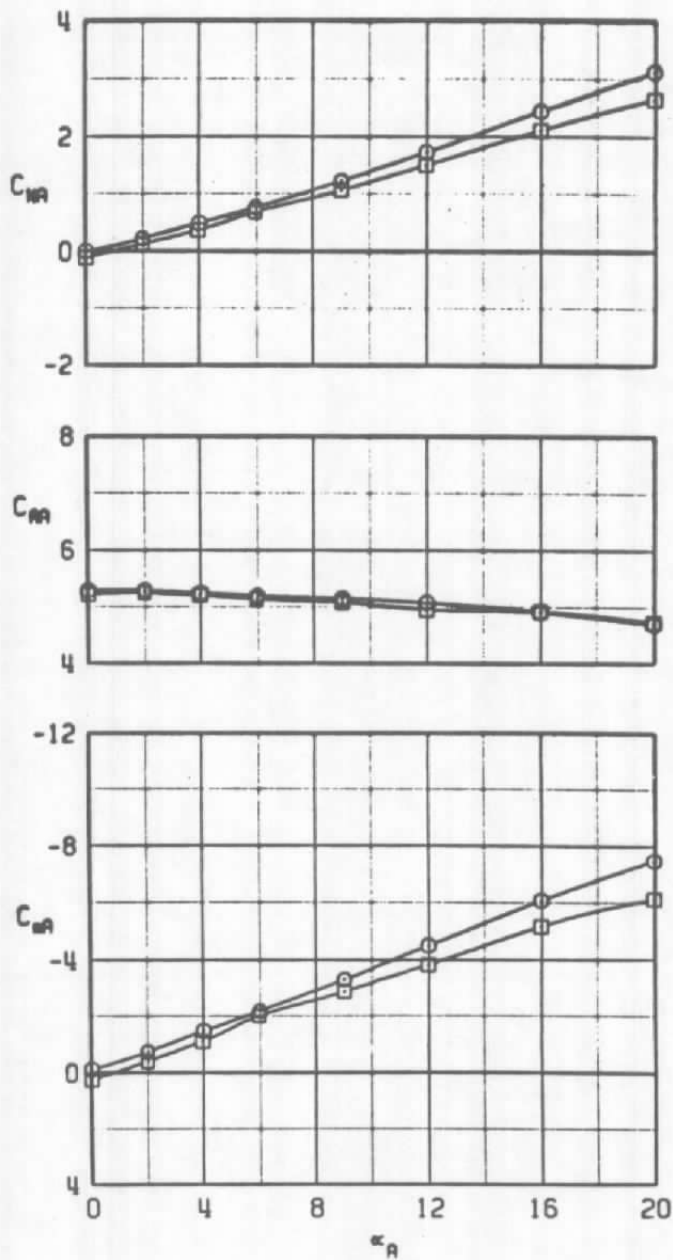
Figure 9. Effects of model roll orientation on the static stability characteristics of the MK-84 with T2 fins,  $\phi_B = -45$  deg.

SYMBOL	$M_\infty$	$\phi_H$
○	0.6	0
□	0.6	-45



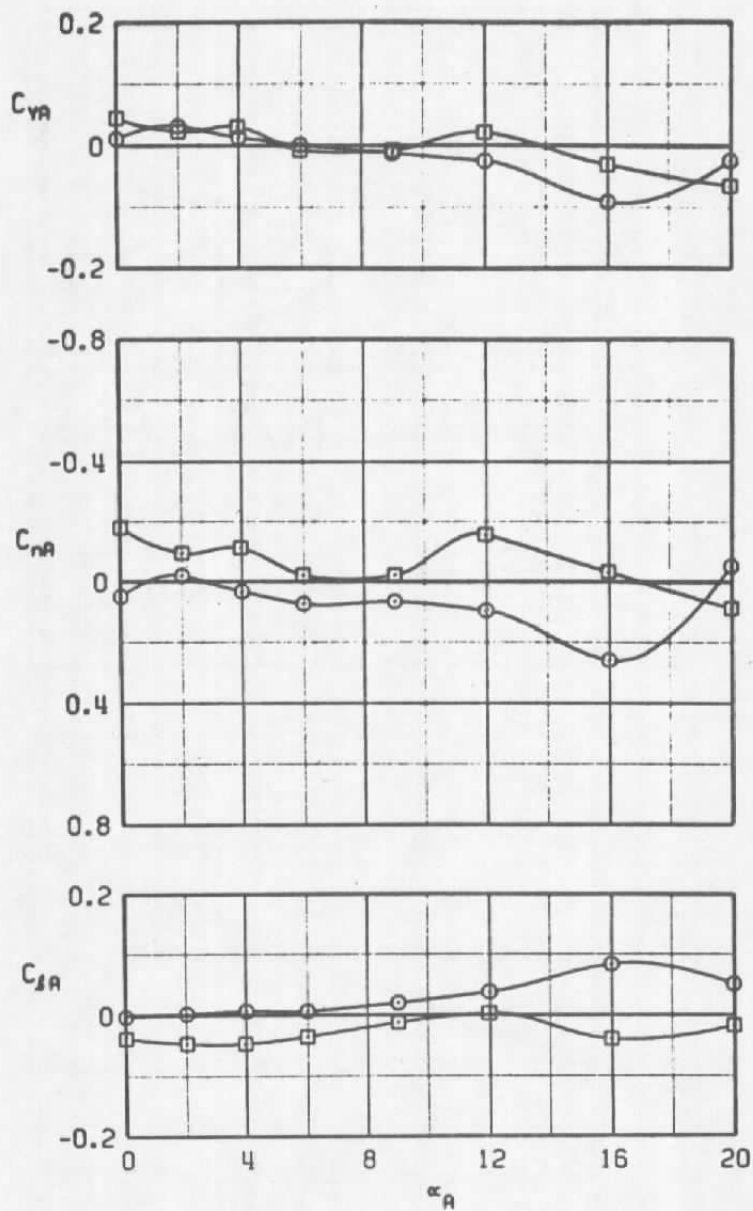
a. Concluded  
Figure 9. Continued.

SYMBOL	$M_\infty$	$\phi_N$
○	0.8	0
□	0.8	-45



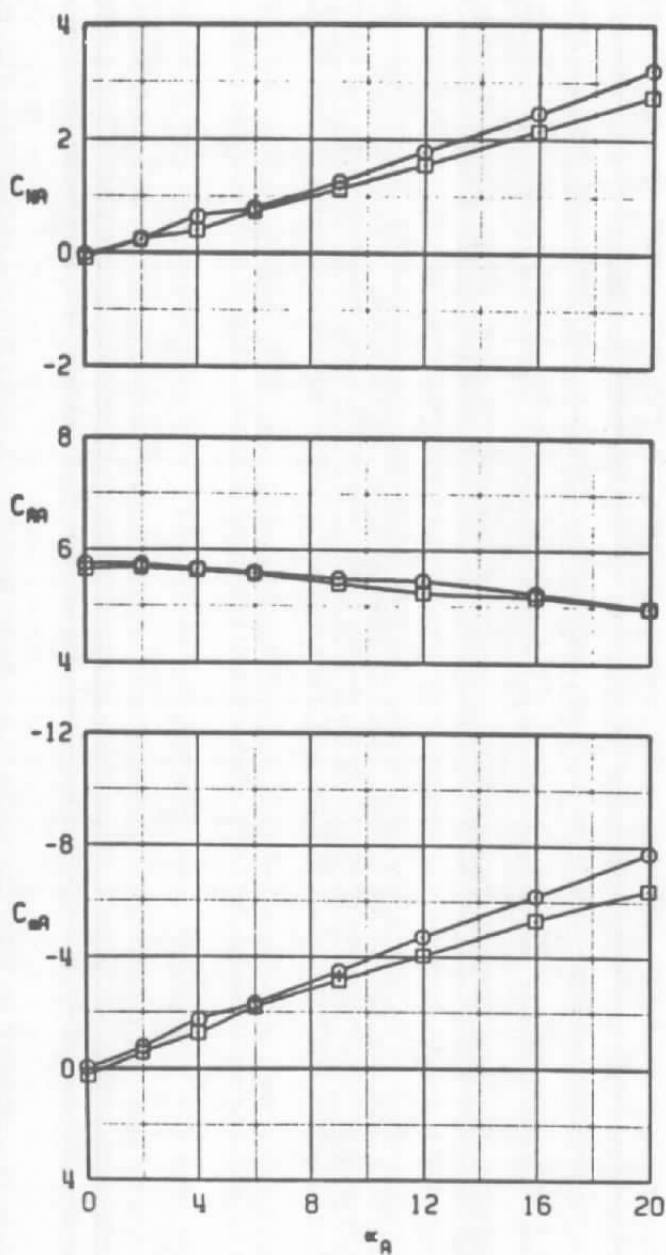
b.  $M_\infty = 0.8$   
Figure 9. Continued.

SYMBOL	$M_\infty$	$\phi_A$
○	0.8	0
□	0.8	-45



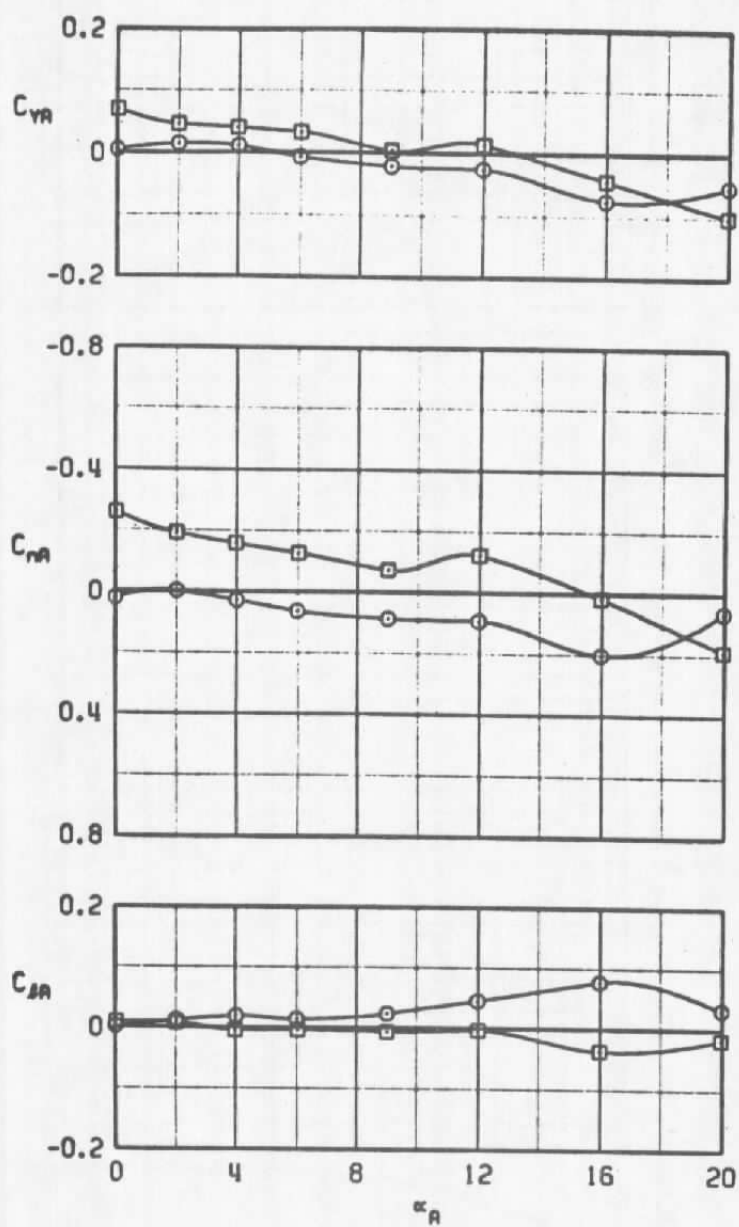
b. Concluded  
Figure 9. Continued.

SYMBOL	$M_\infty$	$\phi_w$
$\odot$	0.9	0
$\square$	0.9	-45



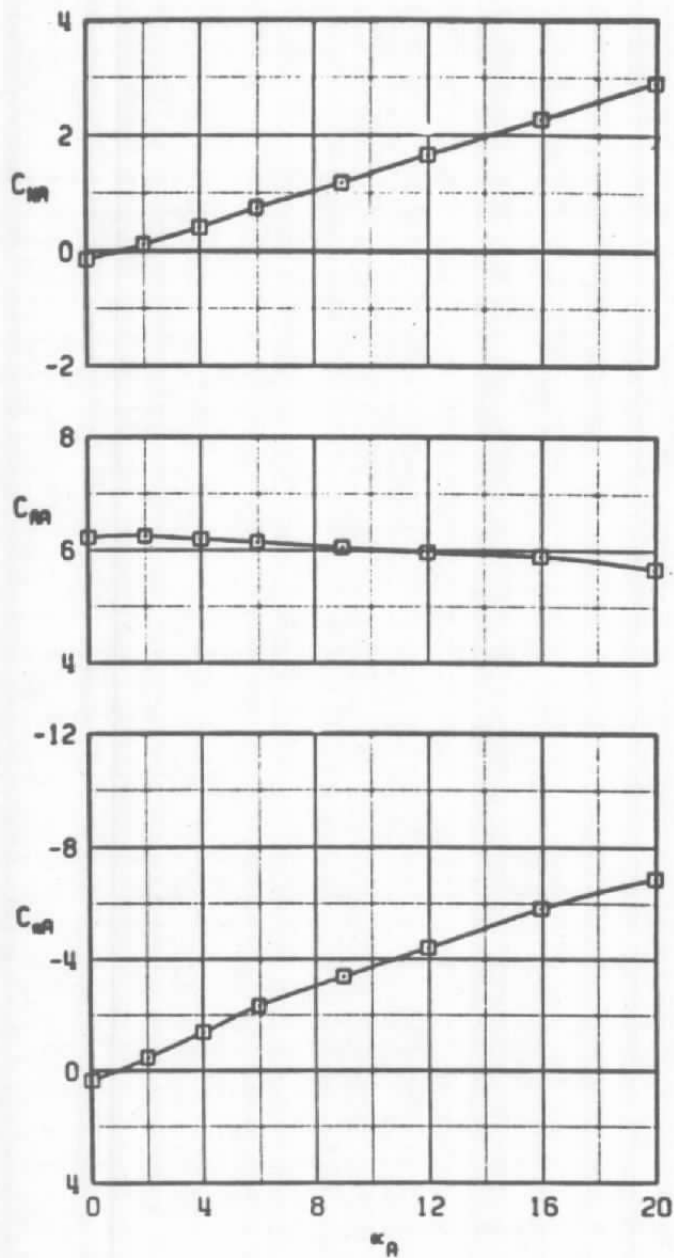
c.  $M_\infty = 0.9$   
Figure 9. Continued.

SYMBOL	$M_\infty$	$\alpha_\infty$
$\circ$	0.9	0
$\square$	0.9	-45



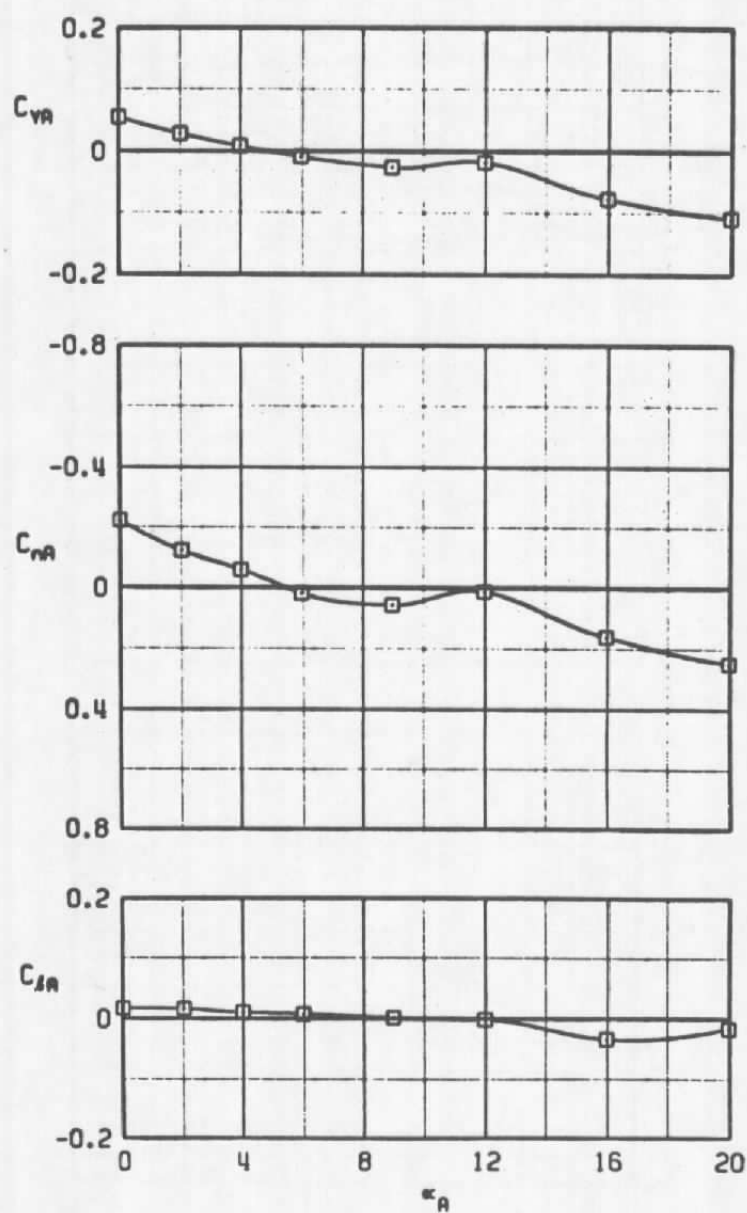
c. Concluded  
Figure 9. Continued.

SYMBOL	$M_\infty$	$\phi_w$
□	1.0	-45



d.  $M_\infty = 1.0$   
Figure 9. Continued.

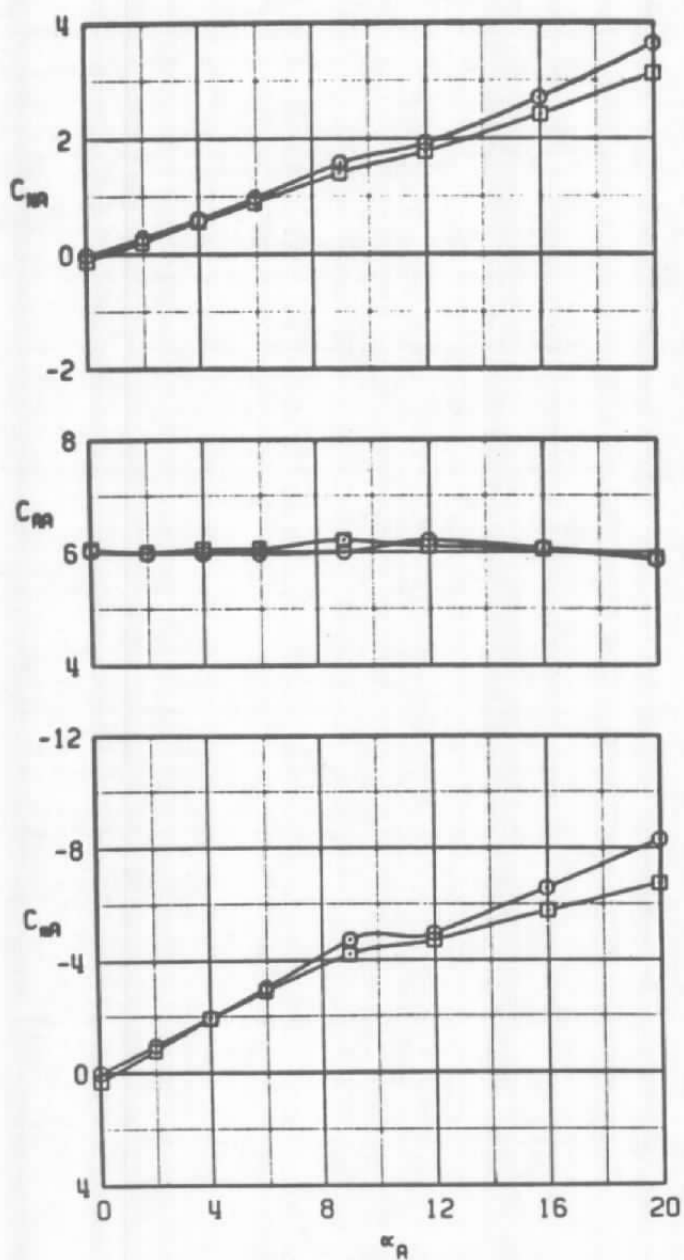
SYMBOL	$M_\infty$	$\phi_n$
$\square$	1.0	-45



d. Concluded  
Figure 9. Continued.

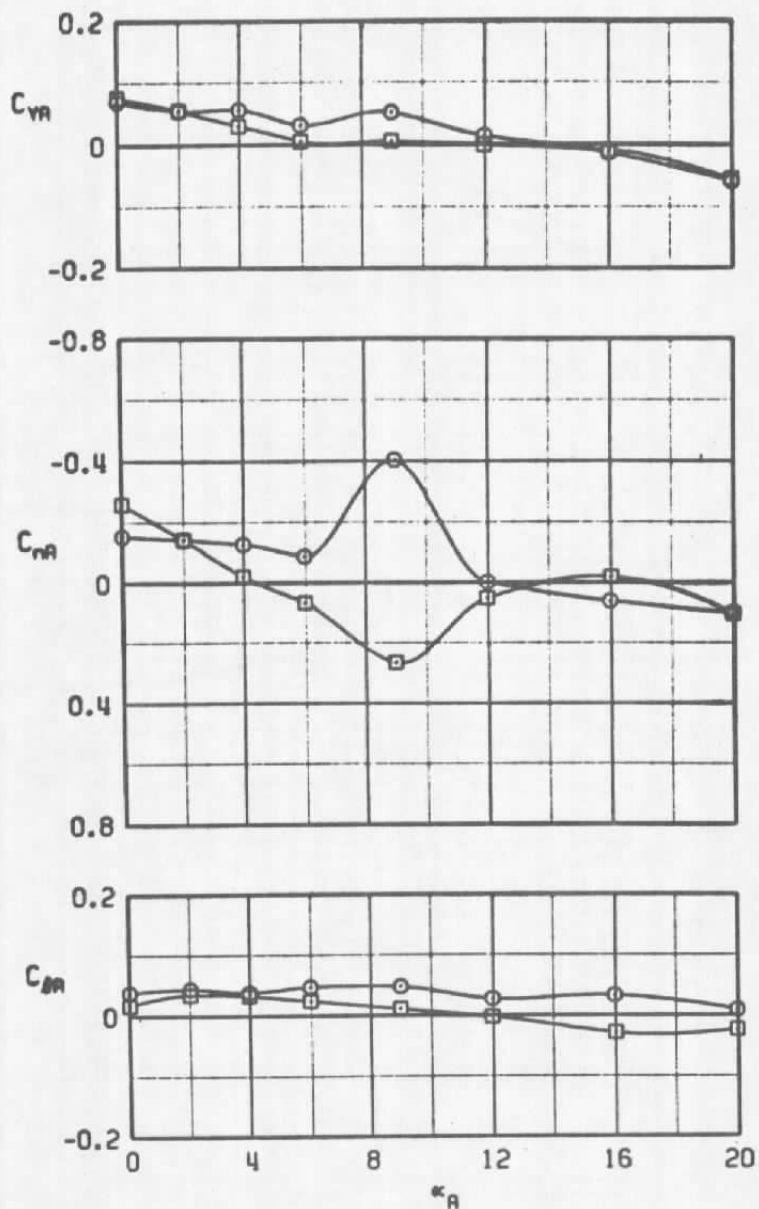


SYMBOL	$M_\infty$	$\alpha_R$
○	1.1	0
□	1.1	-45



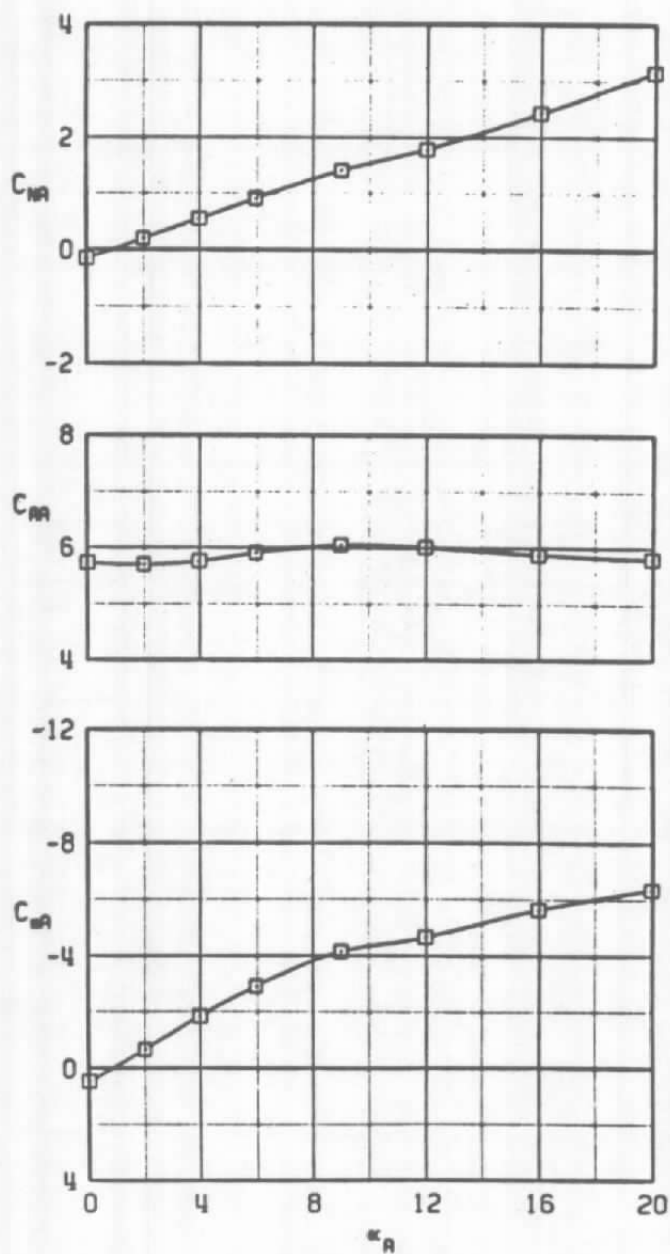
e.  $M_\infty = 1.1$   
Figure 9. Continued.

SYMBOL	$M_\infty$	$\phi_w$
$\circ$	1.1	0
$\square$	1.1	-45



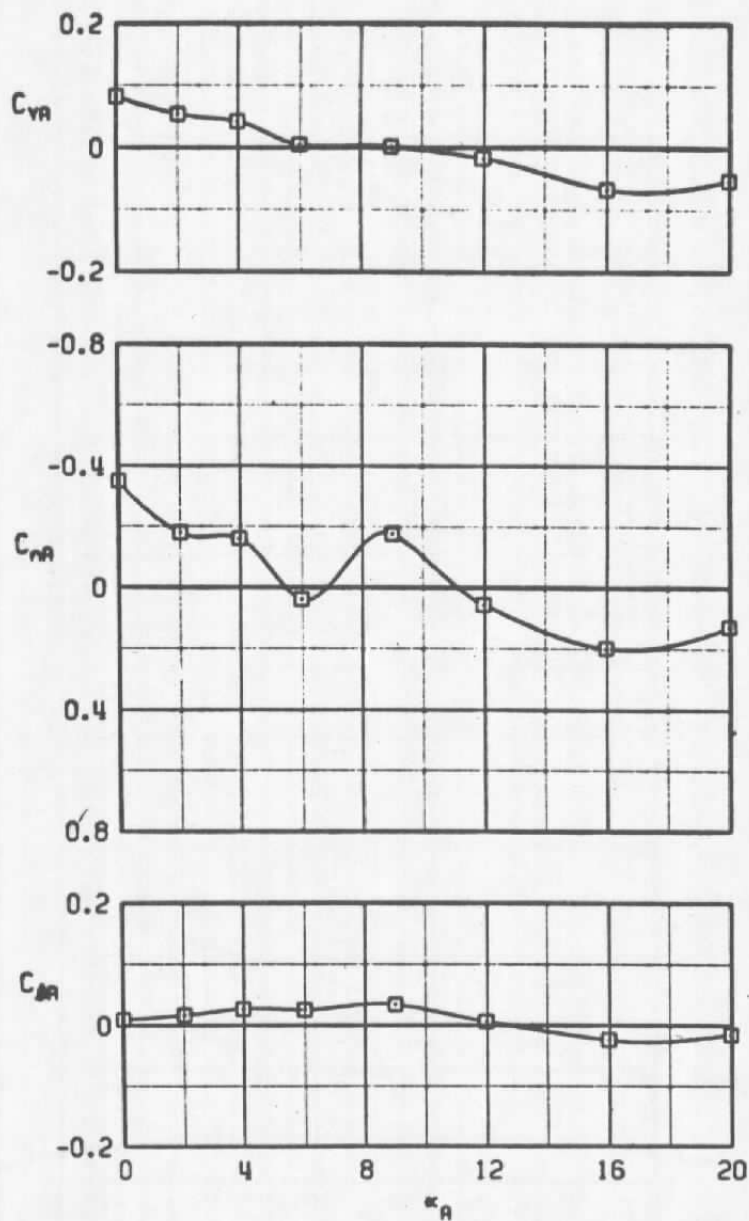
e. Concluded  
Figure 9. Continued.

SYMBOL	$M_\infty$	$\phi_n$
$\square$	1.2	-45



f.  $M_\infty = 1.2$   
Figure 9. Continued.

SYMBOL	$M_\infty$	$\alpha_n$
$\square$	1.2	-45



f. Concluded  
Figure 9. Concluded.

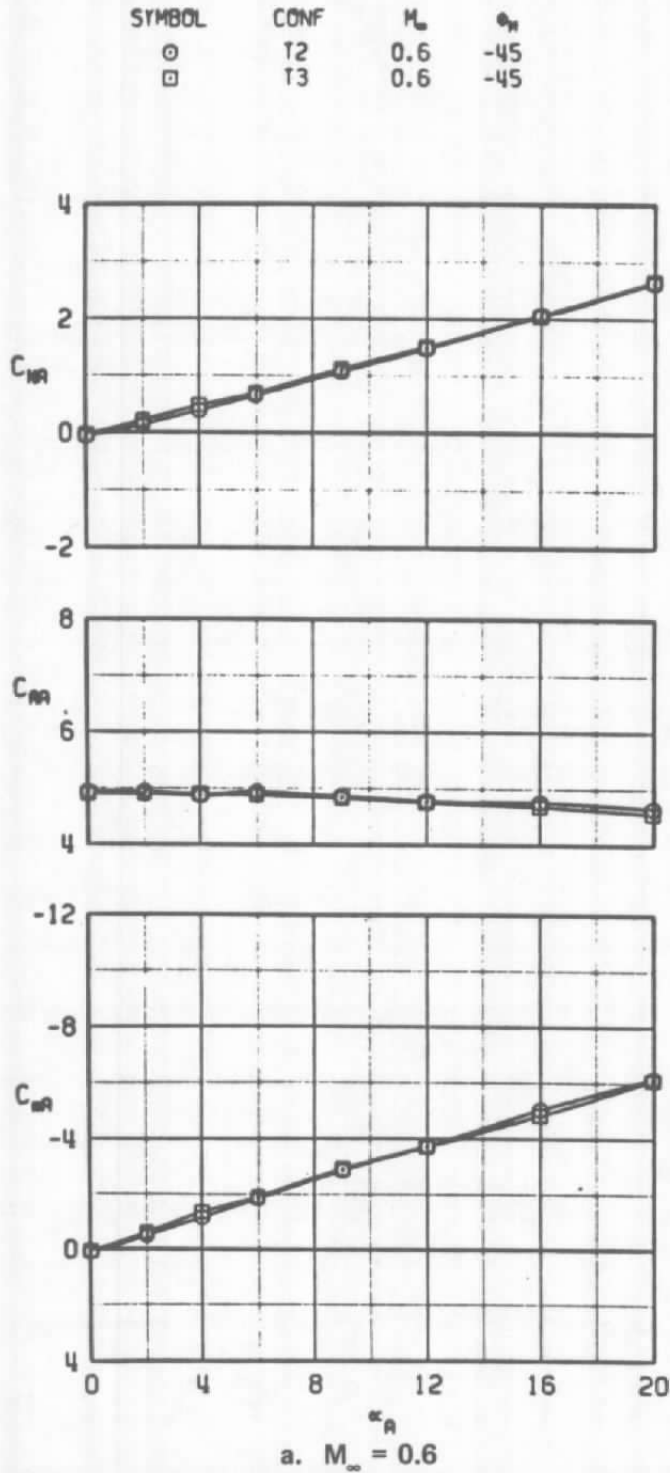
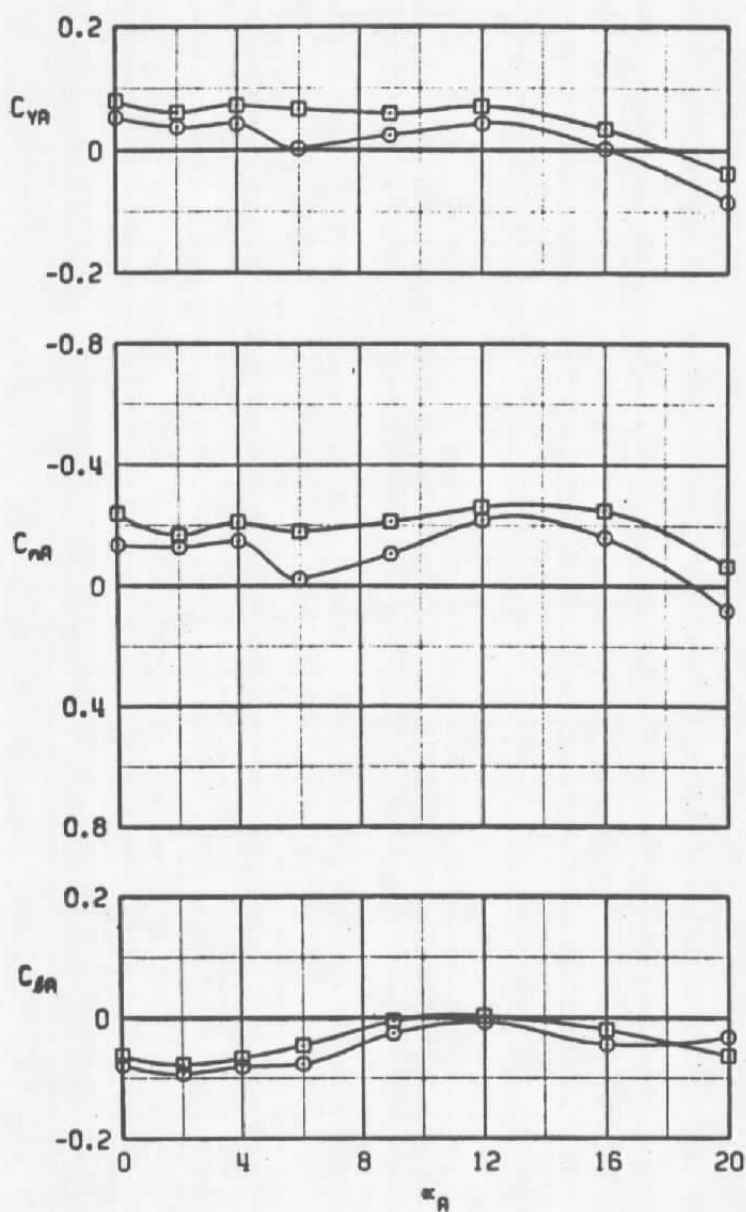


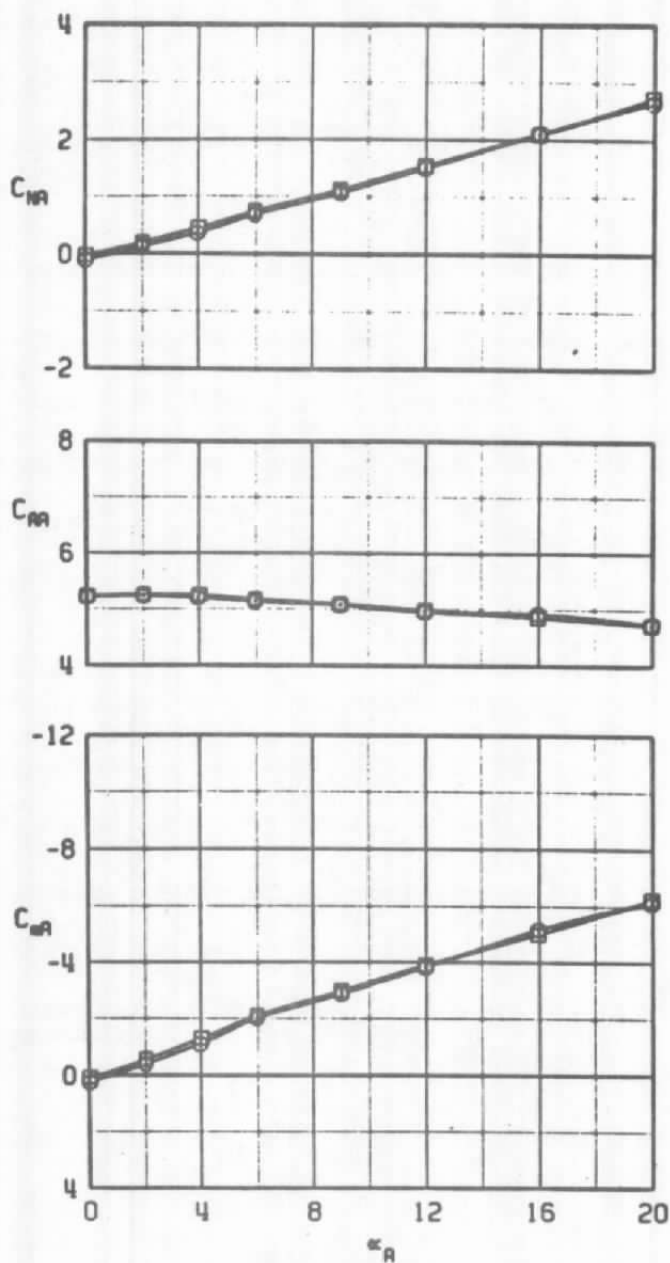
Figure 10. Effects of fin configuration on the static stability characteristics of the MK-84,  $\phi_B$  and  $\phi_M = -45$  deg.

SYMBOL	CONF	$M_\infty$	$\alpha_w$
○	T2	0.6	-45
□	T3	0.6	-45



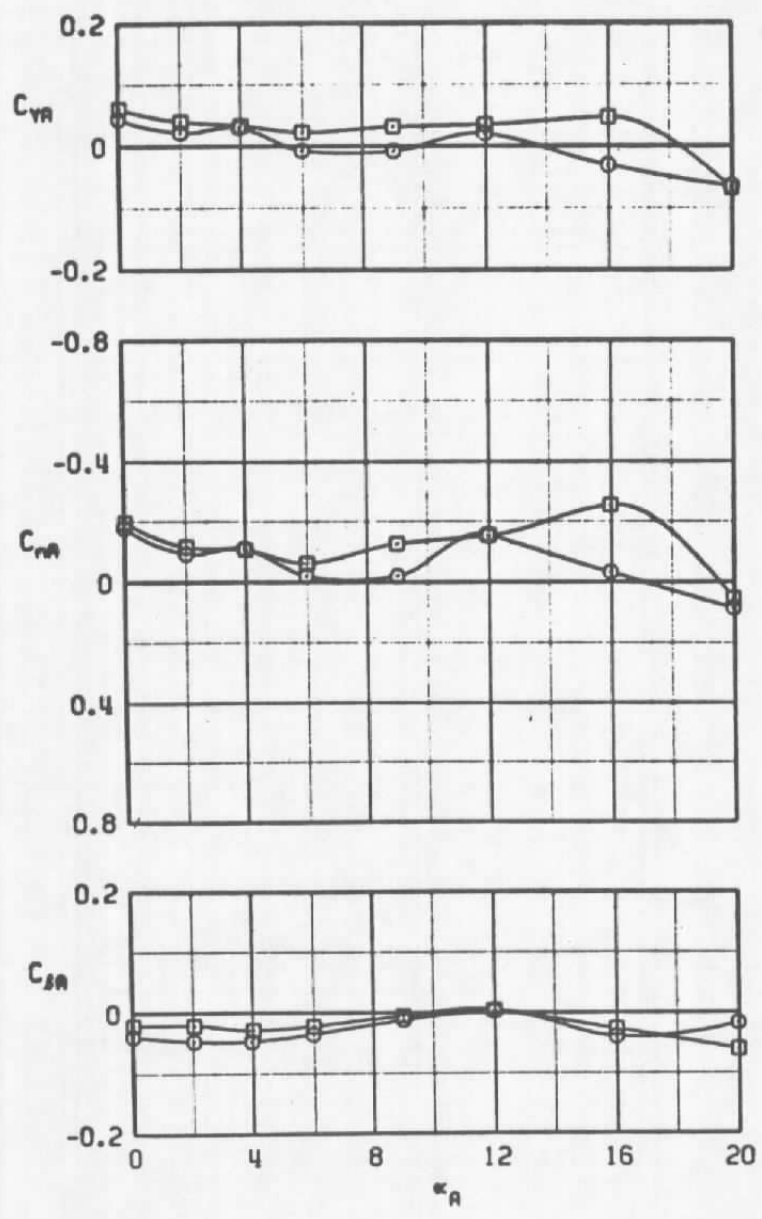
a. Concluded  
Figure 10. Continued.

SYMBOL	CONF	$M_\infty$	$\phi_w$
○	12	0.8	-45
□	13	0.8	-45



b.  $M_\infty = 0.8$   
Figure 10. Continued.

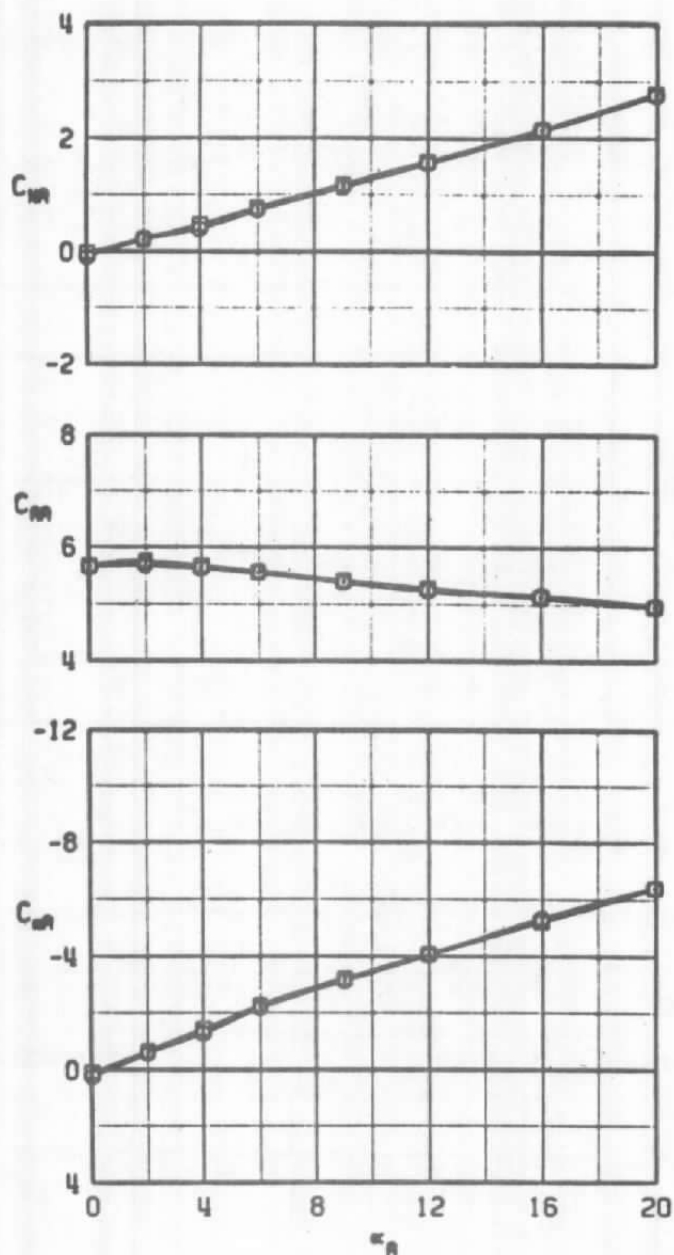
SYMBOL	CONF	M <sub>∞</sub>	α <sub>W</sub>
○	12	0.8	-45
□	13	0.8	-45



b. Concluded  
Figure 10. Continued.

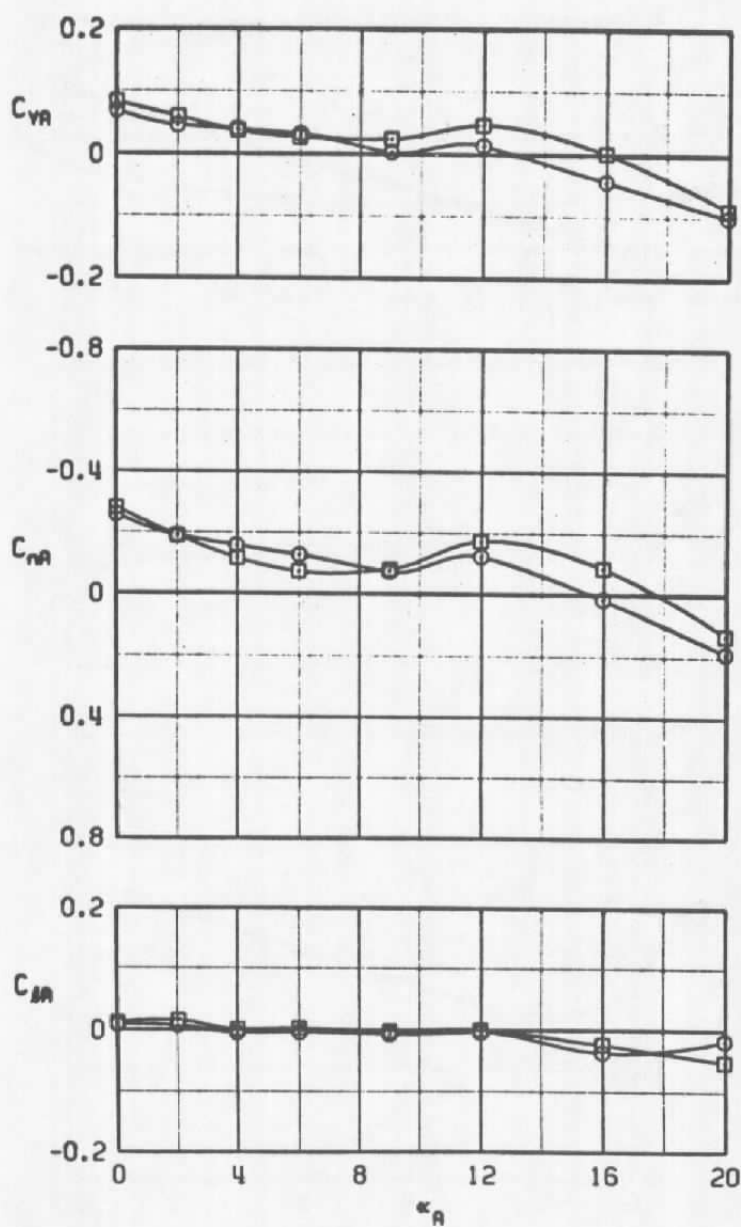


SYMBOL	CONF	$M_\infty$	$\phi_H$
○	T2	0.9	-45
□	T3	0.9	-45



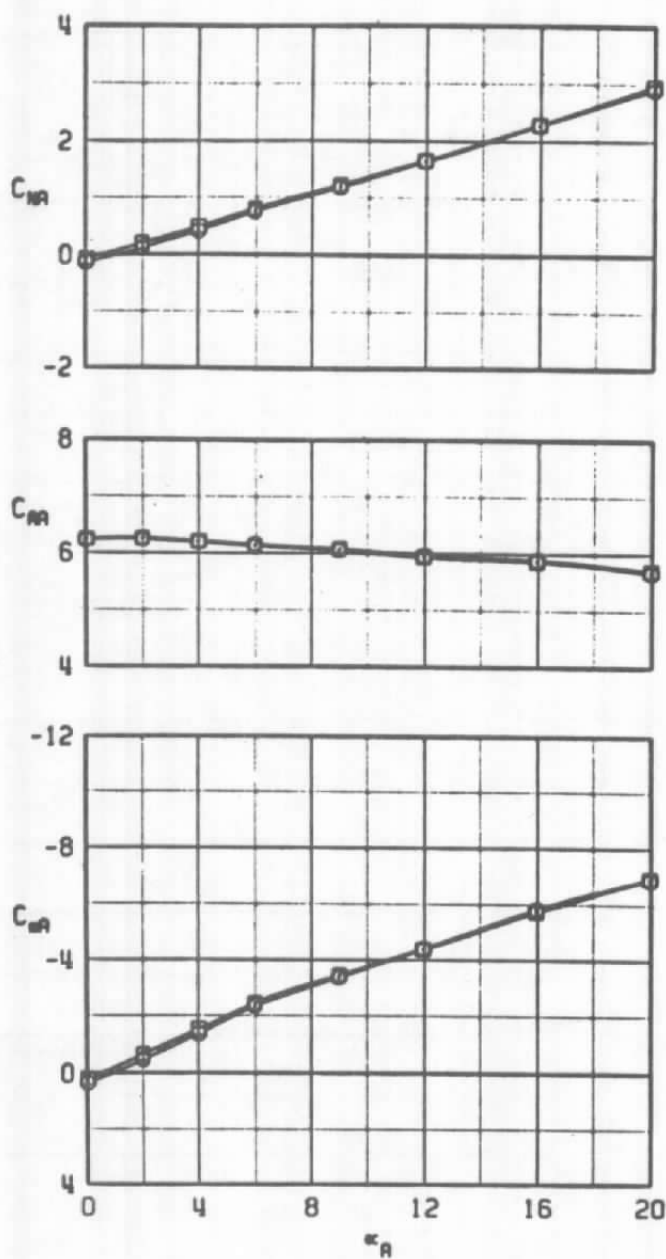
c.  $M_\infty = 0.9$   
Figure 10. Continued.

SYMBOL	CONF	$M_\infty$	$\phi_w$
○	T2	0.9	-45
□	T3	0.9	-45



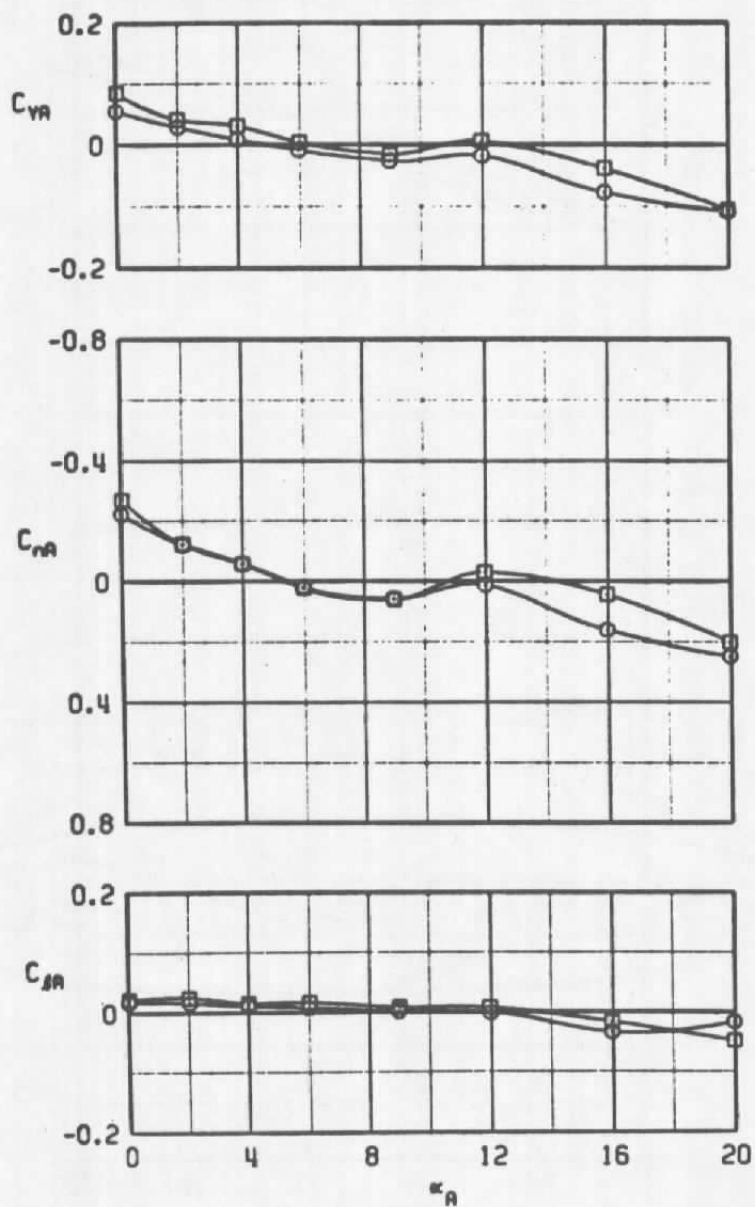
c. Concluded  
Figure 10. Continued.

SYMBOL	CONF	$M_\infty$	$\phi_H$
○	T2	1.0	-45
□	T3	1.0	-45



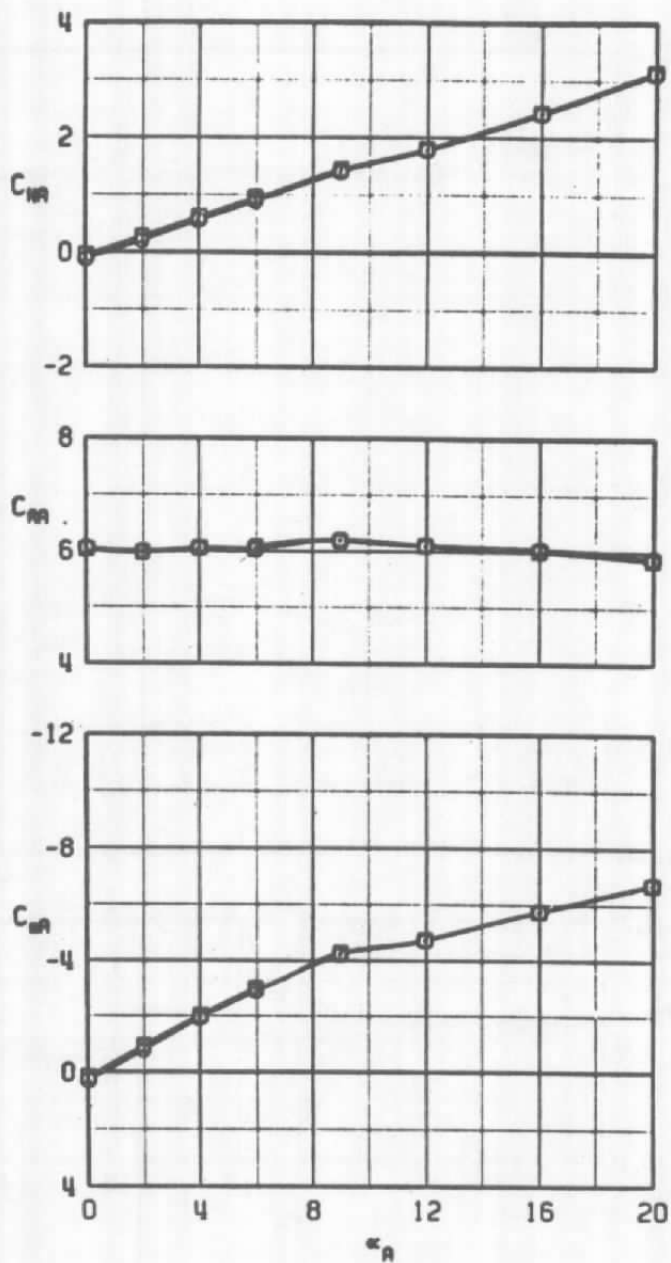
d.  $M_\infty = 1.0$   
Figure 10. Continued.

SYMBOL	CONF	$M_\infty$	$\phi_w$
○	T2	1.0	-45
□	T3	1.0	-45



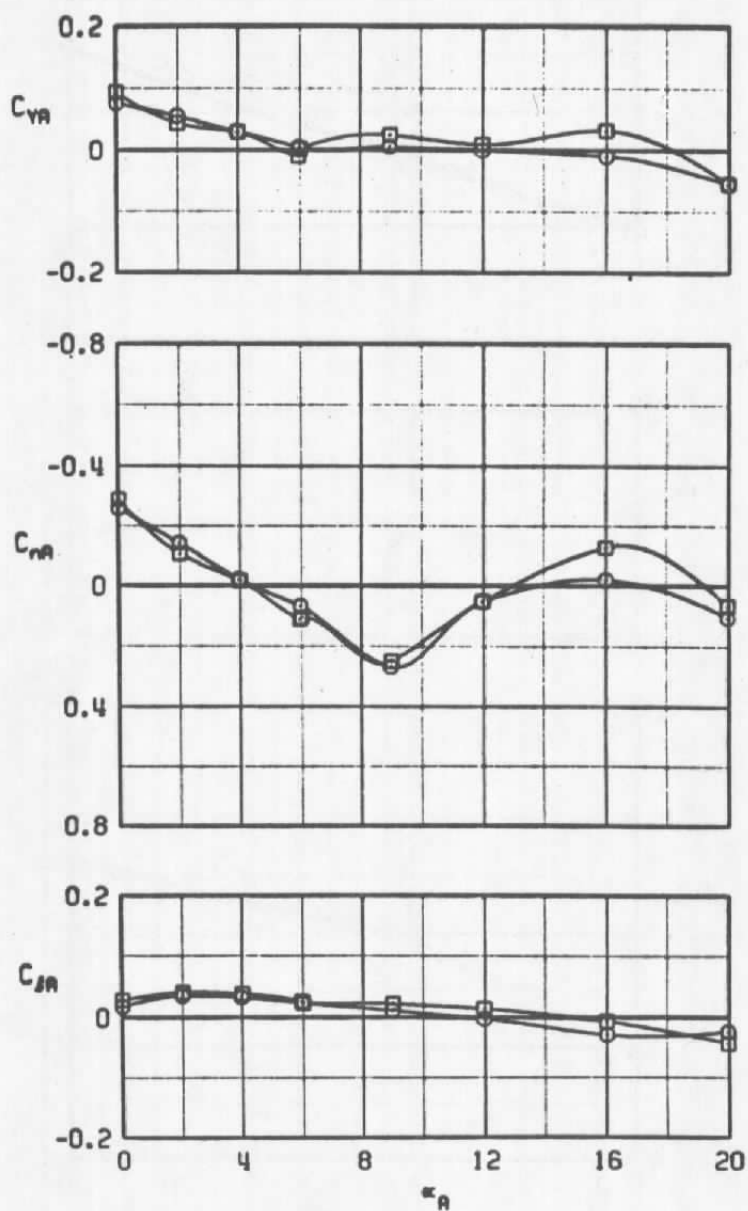
d. Concluded  
Figure 10. Continued.

SYMBOL	CONF	$M_\infty$	$\alpha_N$
○	T2	1.1	-45
□	T3	1.1	-45



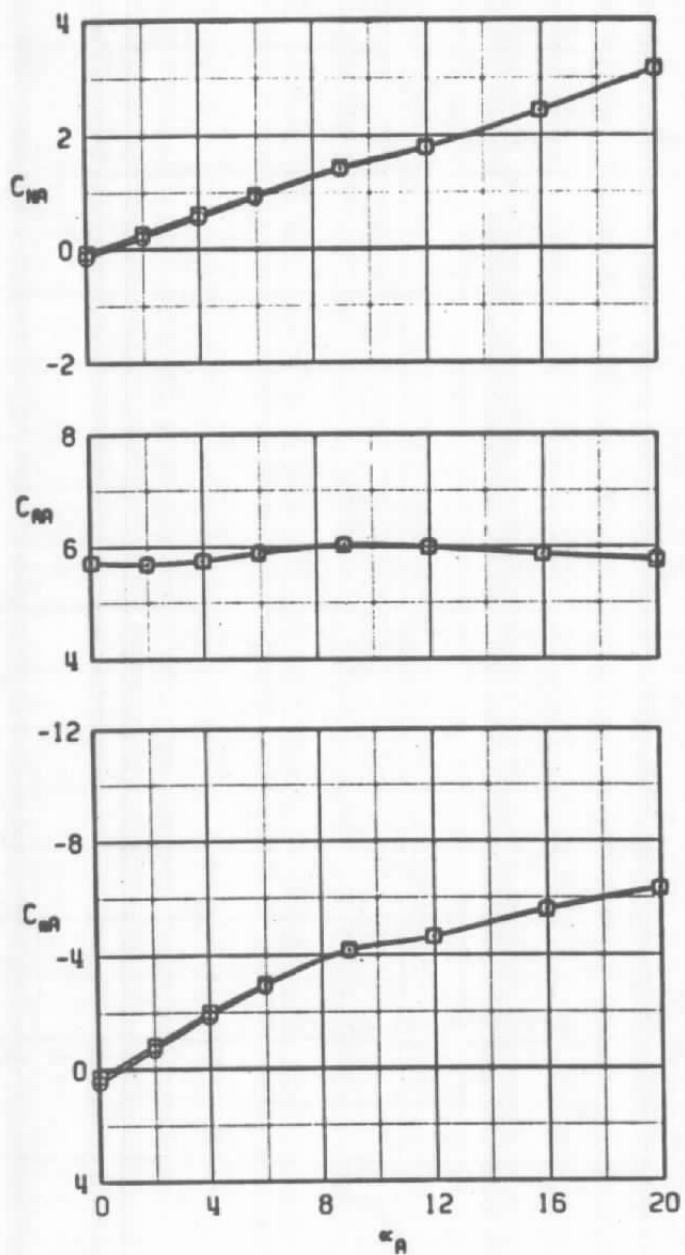
e.  $M_\infty = 1.1$   
Figure 10. Continued.

SYMBOL	CONF	$M_\infty$	$\phi_w$
$\circ$	T2	1.1	-45
$\square$	T3	1.1	-45



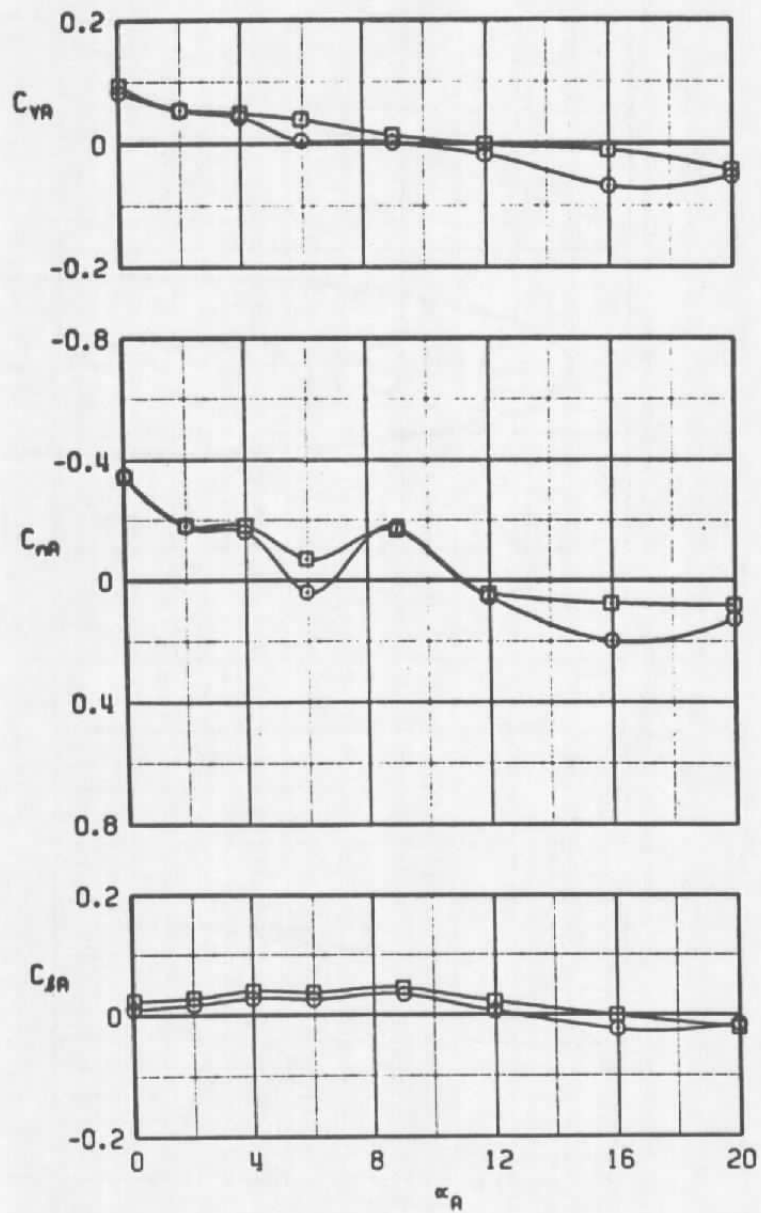
e. Concluded  
Figure 10. Continued.

SYMBOL	CONF	$M_\infty$	$\phi_w$
○	T2	1.2	-45
□	T3	1.2	-45



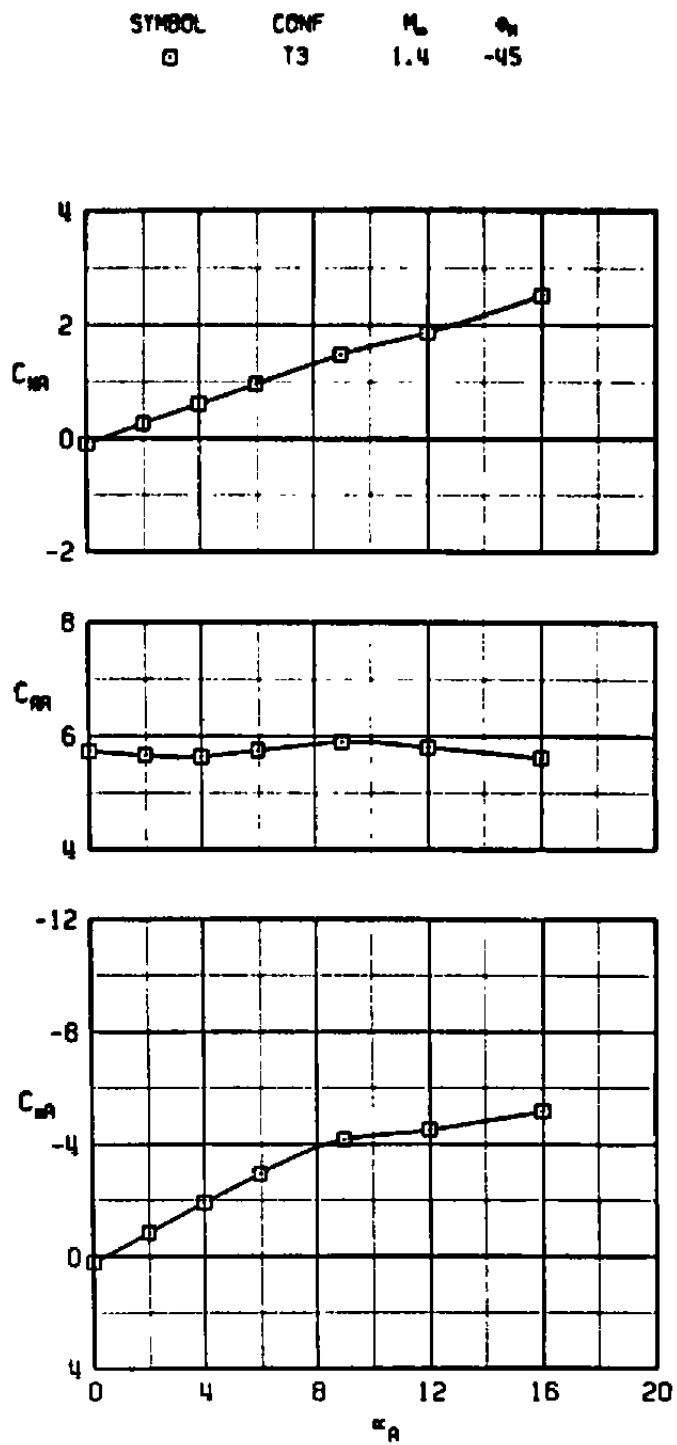
f.  $M_\infty = 1.2$   
Figure 10. Continued.

SYMBOL	CONF	$M_\infty$	$\phi_w$
○	T2	1.2	-45
□	T3	1.2	-45



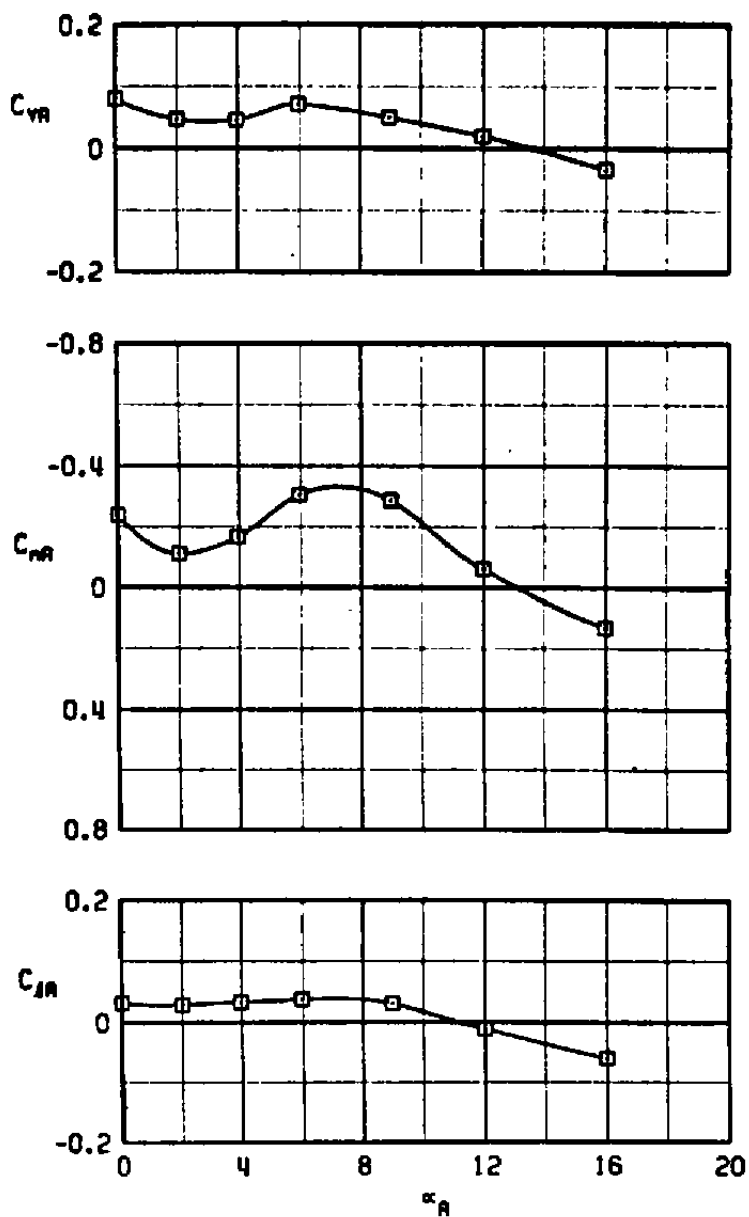
f. Concluded  
Figure 10. Continued.





g.  $M_\infty = 1.4$   
Figure 10. Continued.

SYMBOL	CONF	$M_\infty$	$\phi_n$
$\square$	T3	1.4	-45



g. Concluded  
Figure 10. Concluded.

## NOMENCLATURE

$C_{AA}$	Axial-force coefficient, $F_A/q_\infty S$
$C_{lA}$	Rolling-moment coefficient, $M_l/q_\infty Sd$
$C_{mA}$	Pitching-moment coefficient, $M_m/q_\infty Sd$
$C_{NA}$	Normal-force coefficient, $F_N/q_\infty S$
$C_{nA}$	Yawing-moment coefficient, $M_n/q_\infty Sd$
$C_{YA}$	Side-force coefficient, $F_Y/q_\infty S$
$d$	Reference length, maximum diameter of model centerbody, 0.3958 ft
$F_A$	Measured axial force, lb
$F_N$	Measured normal force, lb
$F_Y$	Measured side force, lb
$M_l$	Measured rolling moment, ft-lb
$M_m$	Measured pitching moment, ft-lb
$M_n$	Measured yawing moment, ft-lb
$M_\infty$	Free-stream Mach number
MS	Model station
$q_\infty$	Free-stream dynamic pressure, psf
Re	Reynolds number based on $d$
$S$	Reference area, 0.1231 ft <sup>2</sup>
$\alpha_A$	Model angle of attack, deg
$\phi_B$	Ballute roll angle, deg
$\phi_M$	Model roll angle, deg